

**FINAL REPORT  
NASA GRANT  
NAG 11-002-086  
JUNE 1976**

**ON THE ELASTIC STABILITY  
OF SHELLS**

**by  
Wilfred H. Horton**

(NASA-CR-148484) ON THE ELASTIC STABILITY  
OF SHELLS Final Report (Georgia Inst. of  
Tech.) 86 p HC \$5.00 CSSL 13M

N76-31568

Unclas  
G3/39 46794



**School of Aerospace Engineering  
GEORGIA INSTITUTE OF TECHNOLOGY  
Atlanta, Georgia 30332**

## SUMMARY

A synopsis of a series of investigations into the instability of axially compressed cylindrical shells is given in this report. There are two prime parts. One which deals with studies which were made on small scale plastic vehicles and one which summarizes the results of tests on large realistically reinforced aluminum alloy circular cylinders of contemporary design.

The objective of the research, which was made with models, was to devise a technique of non-destructive evaluation. The results presented show that, with models at any rate, success was achieved. Probing methods which can be used to determine the locations of weakness and the pertinent instability load levels were devised.

The research on large scale shells was undertaken with a view to determining the critical loads under as uniform a circumferential distribution of axial compressive force as possible. It is clear from the results presented that this objective was closely met.

The complete integration of the methods developed with small vehicles into the work on large scale structures was not attained. The difficulties encountered were primarily due to the mechanical incompatibility of the loading system and the probing systems. Studies made in the final stages of the work showed clearly that these difficulties could be overcome.

### Acknowledgements

The work reported was made possible by a grant from NASA. This support is gratefully acknowledged as are the many referenced and unreferenced contributions from various friends and colleagues. Their stimulating discussions and freely given assistance with the experimental program were invaluable.

Tom Haack, Bud and Marlo Skinner must be accorded a special acknowledgement for without their skill and cooperation the work on large shells would have been much less successful.

A sincere word of appreciation is also due to Nell Blake who gave much needed help in the preparation of the final report.

## List of Contents

1.	Introduction.	1
2.	The Model Shell Programs.	2
2.1.	General Statement	2
2.2.	The Use of the Southwell Technique in Conjunction with Harmonic Analysis.	4
2.3.	An Evaluation Method Based on the Variation of Wall Lateral Stiffness with Axial Load Level.	9
2.4.	An Evaluation Method Based Upon the Variation of Dynamic Mass.	15
2.5.	An Evaluation Procedure Based Upon Combined Loading.	22
2.6.	Conclusion Drawn From the Results of the Non-Destructive Evaluation Program.	25
2.7.	A Parametric Study on Ring Stiffened Shells.	25
3.	Tests on Large Scale Stringer & Ring Stiffened Shells.	32
3.1.	General Remarks.	32
3.2.	Details of the Shells.	32
3.2.1.	Main Body Construction	32
3.2.2.	Main Body Inspection.	33
3.2.3.	Shell End Machining.	30
3.3.	Test Facility.	38
3.3.1.	The Loading and Force Reaction System.	39
3.3.2.	Hydraulic System.	41
3.3.3.	Load Determination.	41
3.4.	The Data Acquisition and Processing System.	41

3.5.	Installation of the Test Vehicle in the Facility.	42
3.6.	Quality and Accuracy Achieved in the Large Scale Shell Program.	44
3.6.1.	Shell Circularity.	44
3.6.2.	Shell End Quality.	46
3.6.3.	Load and Reaction Bearing Surface Quality.	46
3.6.4.	Fit of Shell Ends on the Load and Reaction Bearing Surfaces.	46
3.6.5.	Load Steadiness.	46
3.6.6.	Repeatability.	49
3.7.	Results Obtained.	49
3.7.1.	Non-Destructive Evaluation.	49
3.7.2.	Maximum Load Levels Attained.	52
3.7.3.	Buckling Behavior and Post Buckled Condition.	52
3.7.4.	Load-Strain Relationship.	54
3.7.5.	Line-Load Distribution.	67
3.7.6.	Load Displacement Histories.	72
4.	Conclusions.	72

### List of Figures

- Figure 1. Data Acquisition System Flow Diagram.
- Figure 2. Harmonic Spectrum and Southwell Plot, Shell 1000.
- Figure 3. Harmonic Spectrum and Southwell Plot, Shell 1002.
- Figure 4.  $P_{CR}$  and  $P_{SW}$  Compared to Experimental Loads, Shell 10XX.
- Figure 5. A Schematic Diagram of the Stiffness Probe.
- Figure 6. Stiffness-Axial Load Plots for Unstiffened Circular Shell.
- Figure 7. Rectangular Panel -  $M_D$  vs.  $F$  at 30 Hz.
- Figure 8. Elliptic Shell -  $M_D$  vs.  $F$  at 20 Hz.
- Figure 9. Rectangular Panel - Minimum  $M_D$  vs. Corresponding  $P$ .
- Figure 10. Elliptic Shell - Minimum  $M_D$  vs. Corresponding  $P$ .
- Figure 11. Load-Deflection Plots, Increasing Axial Load, for 220 Degrees Angular Position.
- Figure 12. Critical Lateral Force Behavior Under Axial Compression.
- Figure 13.  $P_{SW}$  vs.  $S_R$ , Non-Uniform Rings, Shell 09XX.
- Figure 14.  $P_{SW}$  vs.  $S_R$ , Non-Uniform Rings, Shell 08XX.
- Figure 15. Ring and Stringer Section
- Figure 16. End Ring Section
- Figure 17. Block Diagram of Circularity Checking System.
- Figure 18. Schematic of Large Shell Testing System.
- Figure 19. Large Shell Initial Geometry.

### List of Tables

- Table I. Summary of the Result of the Wall Stiffness Variation Study.
- Table II. Stiffness Profile on Unstiffened Circular Shell Under Zero Axial Compression.
- Table III. Comparison of Buckling Loads Predicted From Dynamic Mass Variation With Those Achieved on Test.
- Table IV. Characteristics of the Frames and Stringers of the Shells Used in Ford's Parametric Studies.
- Table V. Characteristics of Shells With Uniform Rings and Stringers.
- Table VI. Characteristics of Shells With Non-Uniform Rings and Uniform Stringers.
- Table VII. Fourier Series Coefficients for Deviation Data.  
(Circumferential)
- Table VIII. Fourier Series Coefficients for Deviation Data.  
(Longitudinal)
- Table IX. Geometric Characteristics of Large Shells Tested.
- Table X. Critical Loads and Stresses.
- Table XI. Height of Strain Measurement Planes Above Base Plane.
- Table XII. Shell D. Strains (Micro-inch per inch) at 15% of Critical Load.
- Table XIII. Shell C. Strains (Micro-inch per inch) at 27.4% of Critical Load.
- Table XIV. Shell A. Strains (Micro-inch per inch) at 75% of Critical Load.

- Table XV. Shell B. Strains (Micro-inch per inch) at 98% of Critical Load.
- Table XVI. Shell A. Local Strain Conditions and Critical Loads Derived From Highest Load Level Data.
- Table XVII. Shell B. Local Strain Conditions and Critical Loads Derived From Highest Load Level Data.
- Table XVIII. Shell C. Local Strain Conditions and Critical Loads Derived From Highest Load Level Data.
- Table XIX. Shell D. Local Strain Conditions and Critical Loads Derived From Highest Load Level Data.
- Table XX. Shell A. Centroidal Strains. Local Centroidal Strains Normalized to Mean.
- Table XXI. Shell B. Centroidal Strains. Local Centroidal Strains Normalized to Mean.
- Table XXII. Shell C. Centroidal Strains. Local Centroidal Strains Normalized to Mean.
- Table XXIII. Shell D. Centroidal Strains. Local Centroidal Strains Normalized to Mean.



## 1. Introduction

The ring and stringer stiffened cylinder finds universal application in aerospace structures, and has done so for several decades. However, it is apparent from a review of the current literature that there is a dearth of practical data obtained from tests on realistic scale vehicles. It is pertinent, too, to note that the actual load distribution achieved on test is quite frequently not clearly defined. In fact, only four cases in which load distribution measurements are available seem to be recorded (1, 2, 3, 4) and of these only one appears to refer to a large scale vehicle. As Babcock (5) notes in his review of shell buckling experiments the practice of determining the actual distribution "is probably not more widely adopted due to the discouraging results obtained in most cases."

The intent of the work, herein reported, was to acquire data on realistic scale ring and stringer stiffened circular cylindrical shells liable to general instability under axial compression. From the onset the goal was to attain the highest quality test vehicles and to achieve the best possible circumferential distribution of axial load.

Realistic scale vehicles of good quality are expensive to procure and prepare for test. Thus it is desirable to maximise the amount of information which can be obtained from each specimen. To this end a secondary program was undertaken - the objective to establish a method of non-destructive evaluation of cylindrical shells

under axial compression.

The two programs were run in parallel. Both are summarized in the report. They are dealt with in the order of their completion.

## 2. The Model Shell Programs:

### 2.1 General Statement

As explained in the introductory section, model studies were conducted in an attempt to derive data which would be pertinent to the main program. In particular, to develop methods of failure prediction which would enable us to determine, from relatively low values of the applied force, the region of failure and the critical load. The shells which were used in the various studies made in this program were constructed from plexiglass, an acrylic plastic with a modulus of  $4.5 \times 10^5$  lb/in<sup>2</sup>. In all cases the tests were conducted in a Baldwin Model 120 CS screwjack universal test machine of 120,000 lb. capacity. This machine was modified so that the load indicating system gave an electrical output proportional to the applied load. Strain gages, when used to check uniformity of load distribution for models were of the Hickson self adhesive variety and were supplied by Tinsley Telcon Ltd., London, S.E. 25. The displacement transducers were in all instances of the Hewlett Packard 24 DCDT or 7 DCDT types. Power for the displacement transducers was from Hewlett Packard 6227 B dual D.C. power supplies and the strain gages worked in conjunction with Hewlett Packard power supplies.

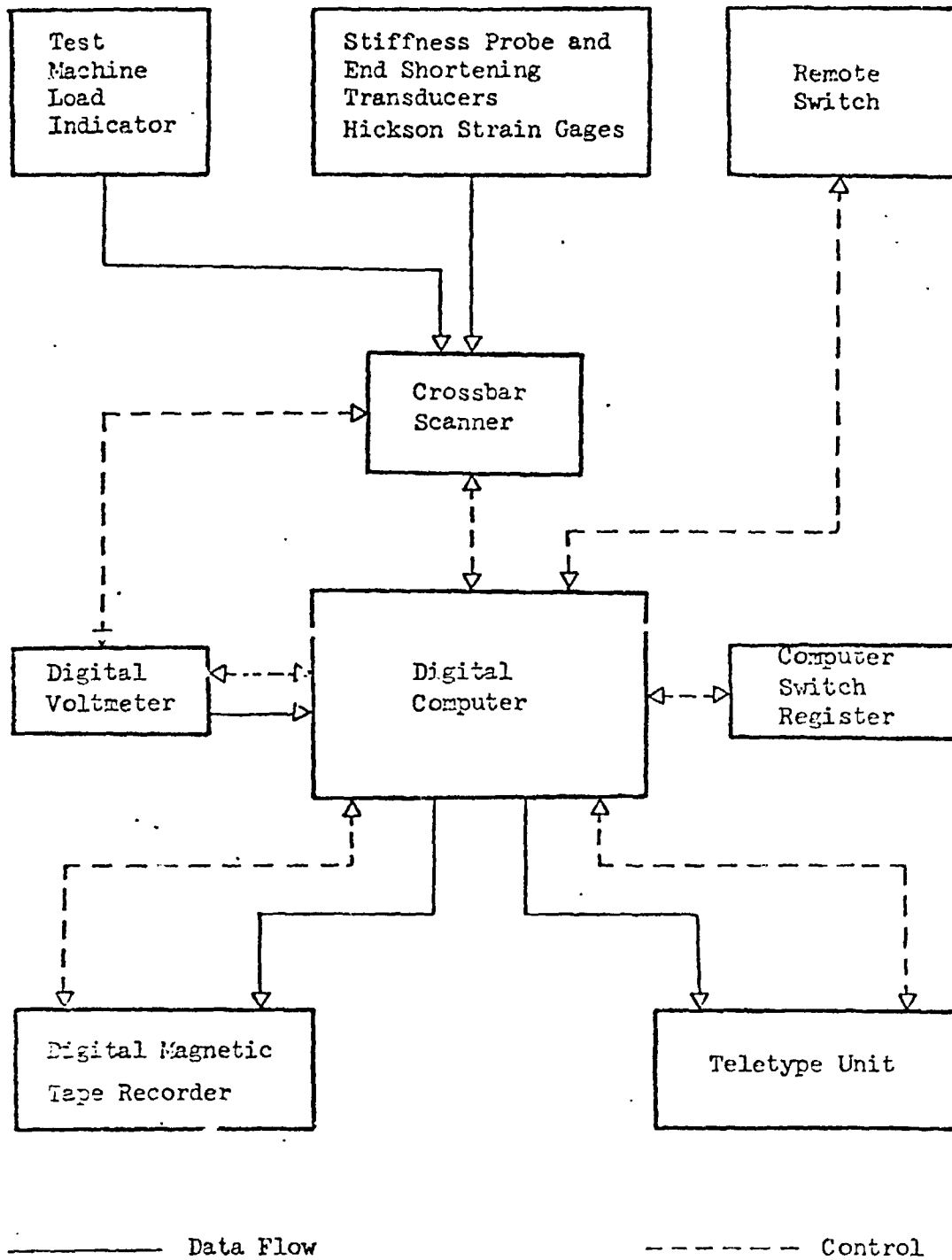


Figure 1 Data Acquisition System Flow Diagram.

The various transducer signals were processed in accordance with the data acquisition system flow diagram given in figure 1. The digital computer therein referenced was of the Hewlett Packard 2115A type, while the digital voltmeter used and the crossbar scanner were compatible Hewlett Packard equipment.

A detailed account of the use of such plastic models for structural research is given in reference 6. Considerable information relative to the method of fabrication is given in reference 7.

## 2.2 The Use of the Southwell Technique in Conjunction With Harmonic Analysis.

The first steps in the non-destructive evaluation program were taken by Ford (8). He started from the observed fact that there is a point - the critical point - for which the normal displacement-load history when analyzed in the Southwell fashion yields a reliable estimate of the instability load. However, the search for such a specific point is a most tedious operation. The question which he sought to resolve was; can a more gross picture of the displacement be treated in such fashion as to obviate the need to locate the critical point? In his attempt to answer this question Ford determined the load-displacement histories at a large number of points on a variety of axially compressed cylindrical shells. He found that when the displacements along a generator were treated as a whole there was considerable uncertainty in the analysis, although Southwell plots could frequently be developed. However, when the displacements

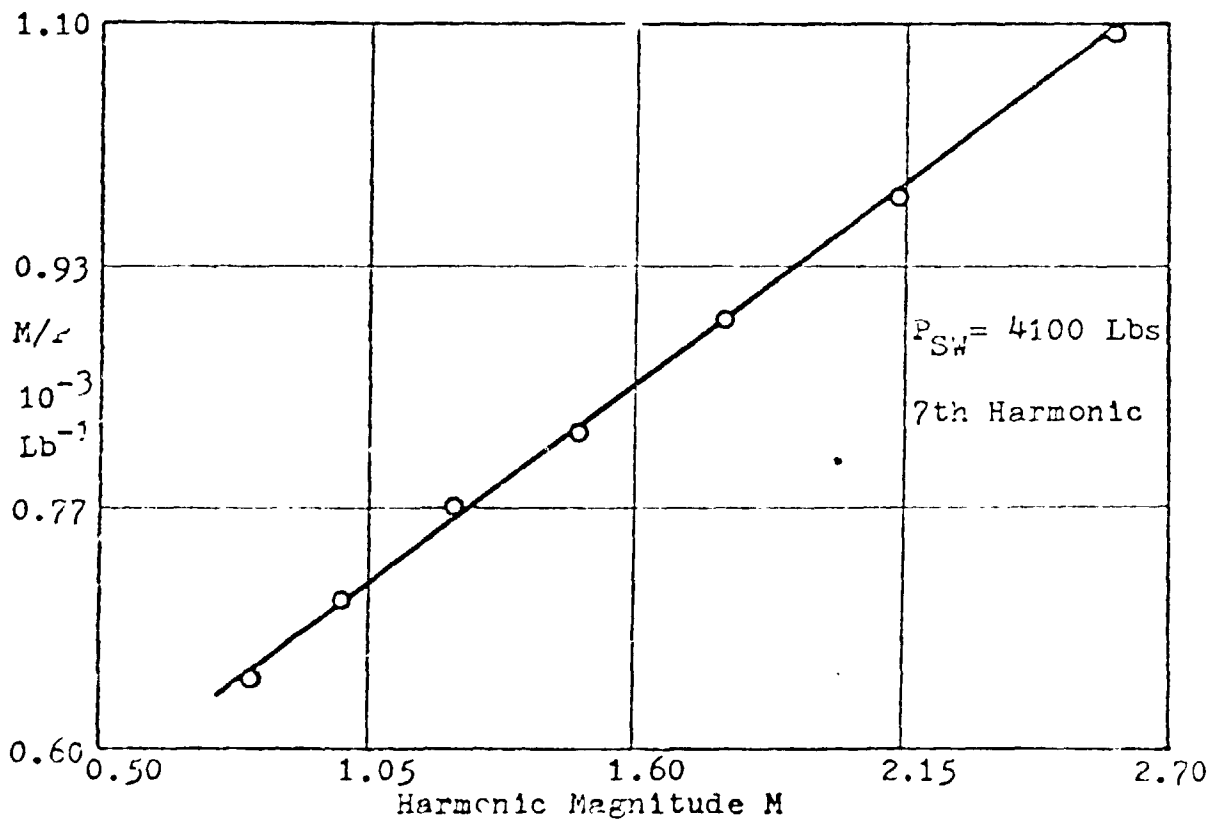
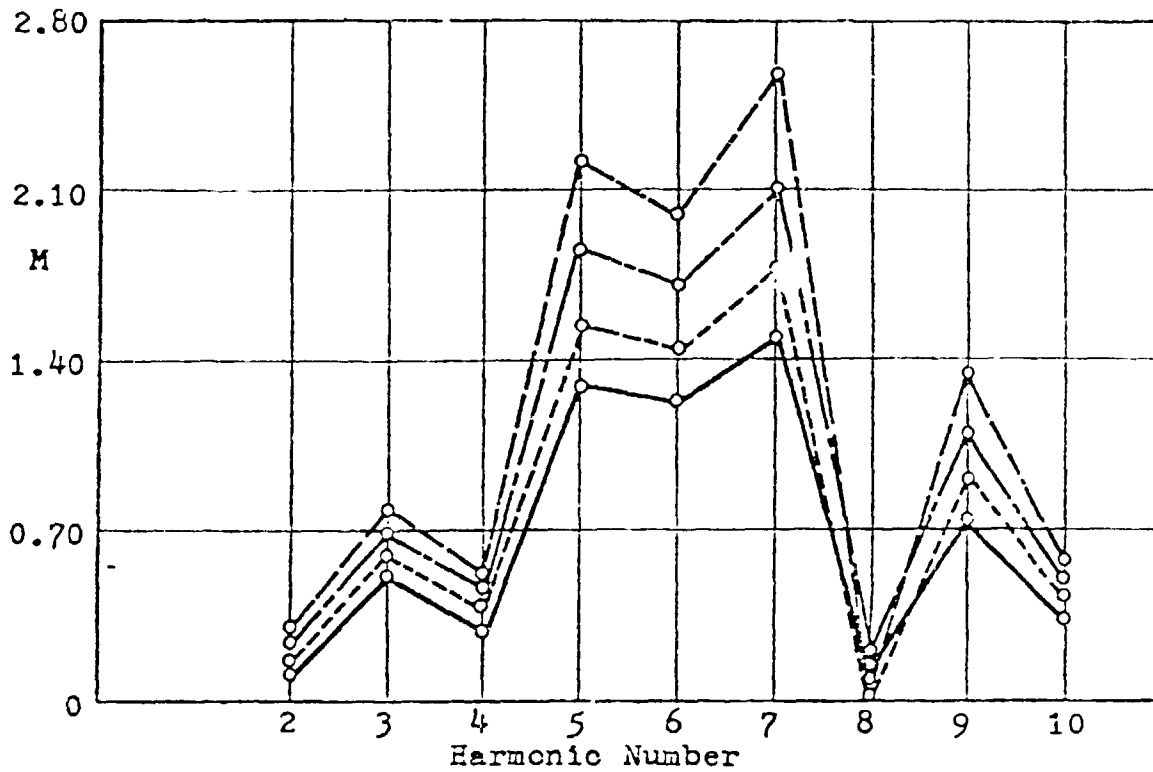


Figure 2 Harmonic Spectrum and Southwell Plot, Shell 1000.

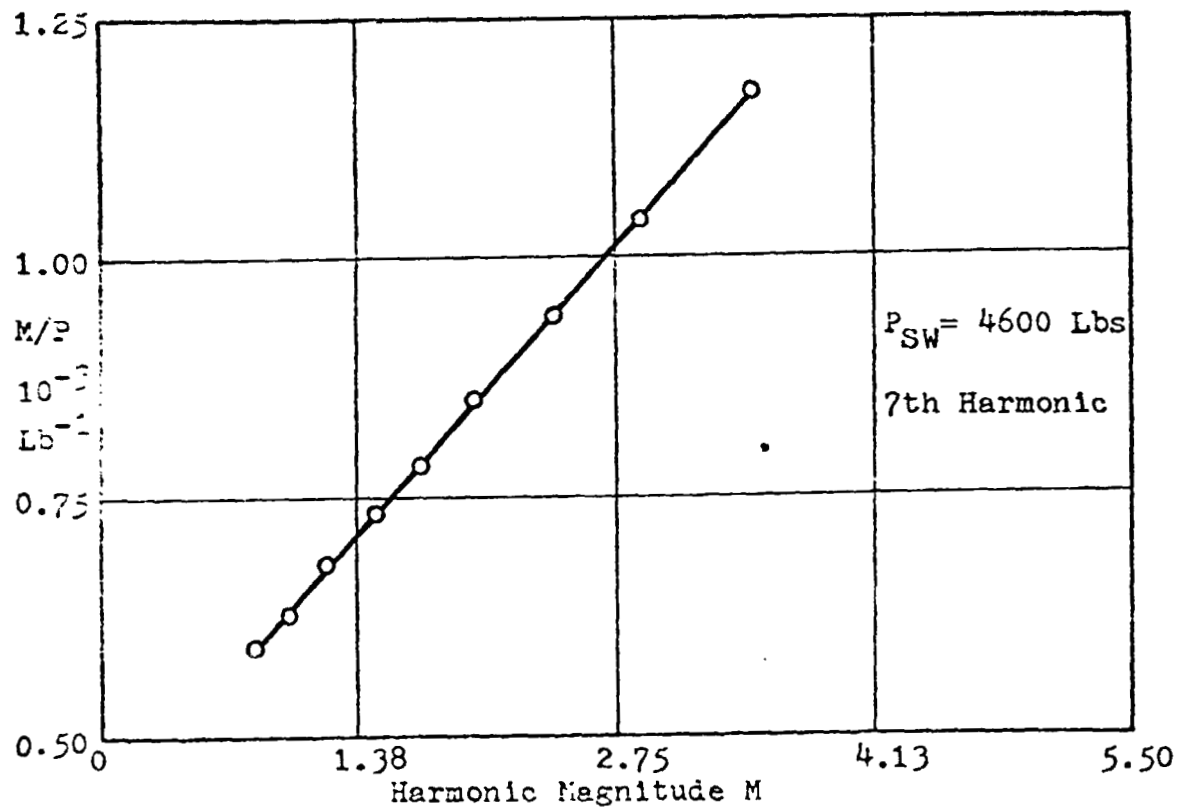
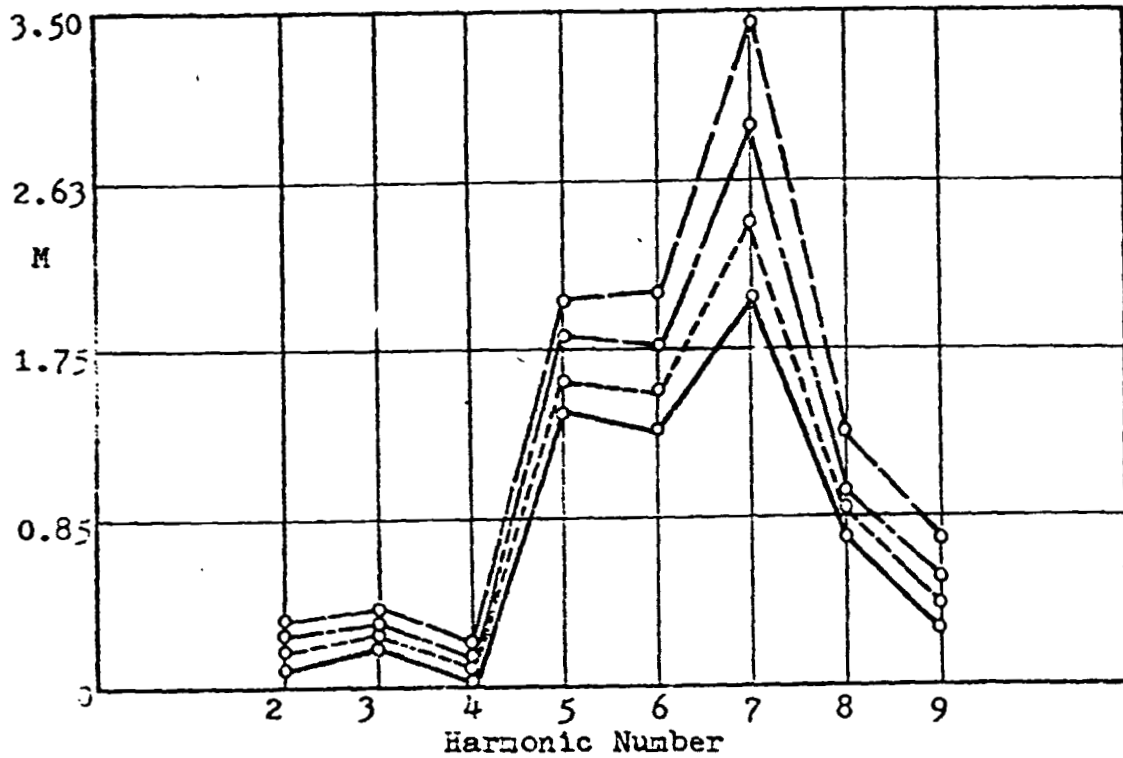


Figure 3 Harmonic Spectrum and Southwell Plot, Shell 1002.

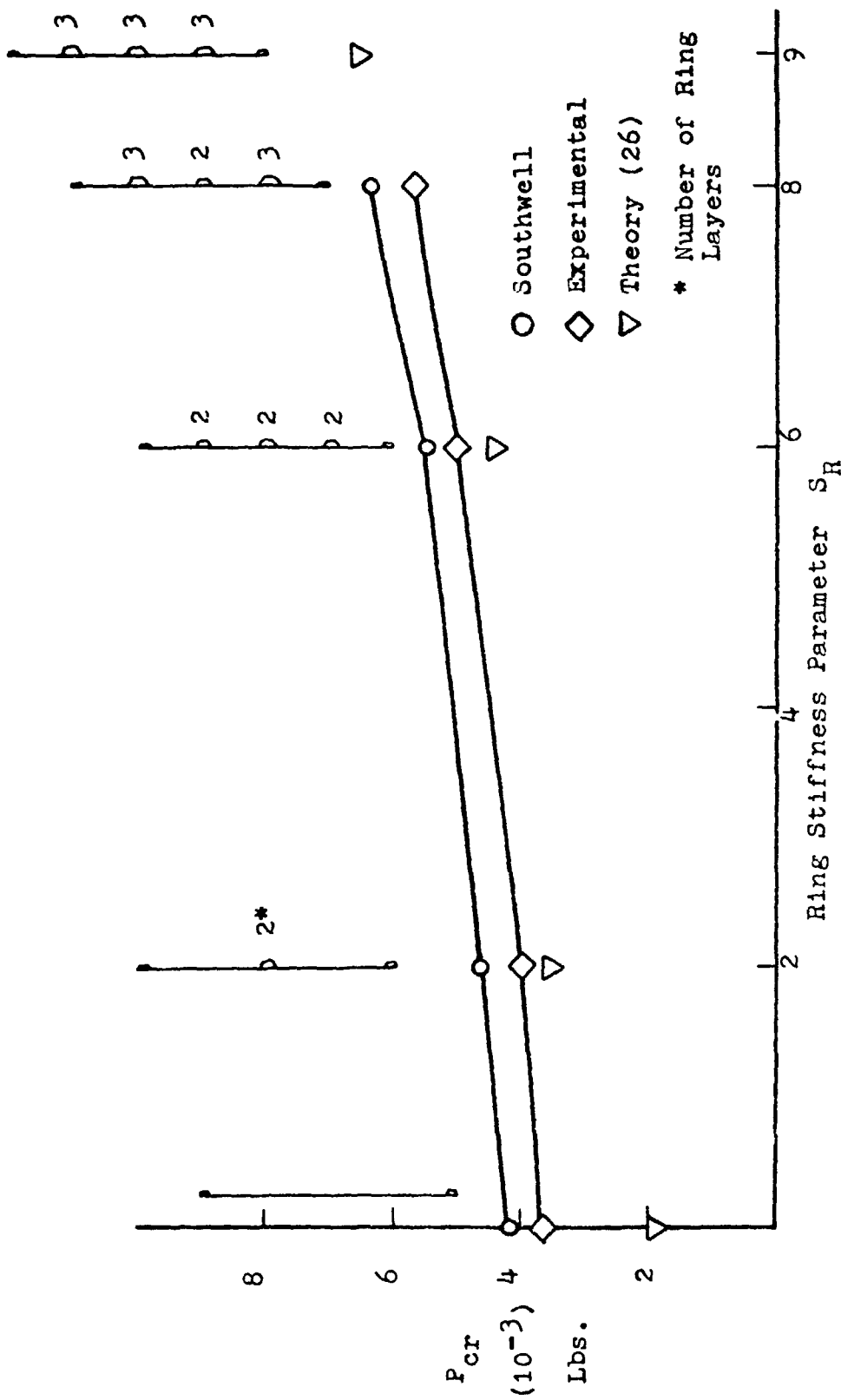


Figure 4.  $P_{cr}$  and  $P_{sw}$  Compared to Experimental Loads, Shell 10XX.

around the shell, in a plane normal to the generators, were considered as a family the ambiguity could be removed. In dealing with the circumferential displacements Ford's procedure was to harmonically analyze the displacement pattern and then to treat the magnitude of the predominant harmonic as a displacement. When this was done excellent Southwell plots could be developed. Fig. 2 & 3 are illustrative of his results. These figures give typical examples of the impulse spectrums and the Southwell plots derived therefrom. For clarity the impulse peaks for the spectrum have been connected by straight lines to form an envelope.

As noted earlier this procedure, which is closely akin to that suggested by Donnell (9), adopted by Tuckerman (10) and applied by Craig (11), removed the ambiguity in interpretation of any particular set of circumferential displacement data. Unfortunately, the location of the vertical stations at which the data should be collected and analyzed was still an open question. For shells of the types used, the indications were that planes in the mid-region were appropriate. Figure 4 gives a comparison of the correspondence between the critical values derived from this procedure, the actual instability load and the predicted values for a specific family of shells. Further details are given in section 2 in which a summary of the total study carried out is presented.

The disadvantages of the method are clear; it involves a considerable amount of analysis and it fails to give any clear indication of the regions of weakness. Moreover the data appropriate is generated only at loads which are a high percentage of the actual critical.



### 2.3 An Evaluation Method Based on the Variation of Wall Lateral Stiffness With Axial Load Level.

A significant weakness of the harmonic analysis technique became clear when consideration was given to data obtained from tests on elliptic shells. Another weakness is that the better the quality of vehicle the higher the load level needed to generate pertinent data. Consideration of these two issues led to a search for a more powerful process which could be universally applied. The first step in this direction was made by Bank (12). He showed that the wall lateral stiffness of a stringer-stiffened circular cylindrical shell decreased as the axial load increased and that there existed at least one point on the shell wall for which this change was linear, and for which the intercept of the load stiffness line with the load axis corresponded to the actual test value of critical load. This observation was made on a single shell.

Singhal (13) extended the work and demonstrated its validity for a wider range of test vehicles.

The six additional types were as follows:

- (1) An unstiffened circular.
- (2) A longitudinally stiffened circular.
- (3) A longitudinally and circumferentially stiffened circular.
- (4) An unstiffened elliptic.
- (5) An unstiffened elliptic with cut-out.
- (6) A spirally stiffened circular.

Special details of these shells and that used by Bank are Given in Table I.

For all of Singhal's tests the normal force used for wall lateral stiffness determination was limited to a level which at zero compression deflected the wall no more than one third its effective thickness and which under load did not cause displacements greater than one half this thickness. The probe used was as shown schematically in Figure 5. Investigation stations were spaced 1.0 inches apart in both the longitudinal and circumferential directions. Singhal was able to show the applicability of the method for orthodox shells but not for spirally stiffened shells.

Figure 6 and Table II give typical data. The minor discrepancy in stiffness values quoted in the table and given on the curve is due to some very slight slop in the turntable bearing.

The advantages of the method are readily apparent.

1. For orthodox reinforcement the cross-sectional shape does not influence the result.
2. It enables the investigator to locate the areas of weakness and to make reliable estimates of critical load from data obtained at relatively low levels of applied end load.

The disadvantages are equally clear.

1. A considerable amount of test time is involved.
2. Special arrangement must be made for the stiffness determination. These involve arrangements for the application of the side force needed and means for determination of the wall displacement, unadulterated by any rigid body motion of the test vehicle.

TABLE I. SUMMARY OF THE RESULT OF THE WALL STIFFNESS VARIATION STUDY

Specimen Number	Shell Construction	Level of Side Force Used (Grams)	Predicted Buckling Load (lb)	Actual Buckling Load (lb)	% Error	Remark
0	Stringer Stiffened Circular	454.	4200	4050	+3.7	Bank's Test. Buckled Elastically
1	Unstiffened Circular	200	1390	1375	+1.1	Buckled Elastically
2	Stringer Stiffened Circular	200 & 500*	1060	1080	-1.9	Buckled Elastically
3	Ring and Stringer Stiffened Circular	500	1950	2000	-2.5	Buckled and Cracked
4	Unstiffened Elliptic	75	360	371	-3.0	Buckled Elastically
5	Unstiffened Elliptic With A Cutout	75	180	191	-5.8	Buckled Elastically
6	Spiral Stiffened Circular	600	4700	3400	+38.2	Buckled and Cracked

\* The differential stiffness was measured in this case

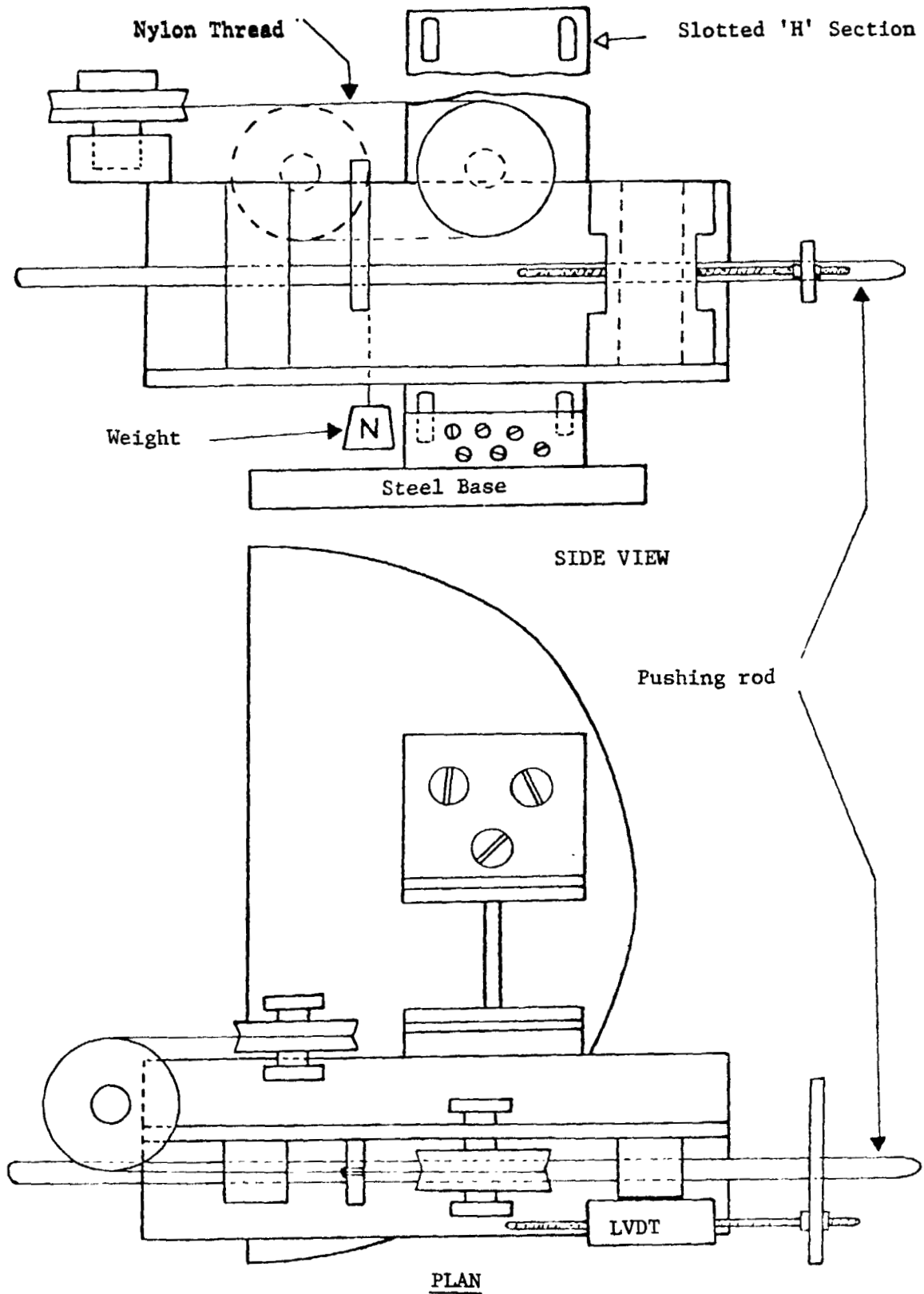


Figure 5. A Schematic Diagram of the Stiffness Probe

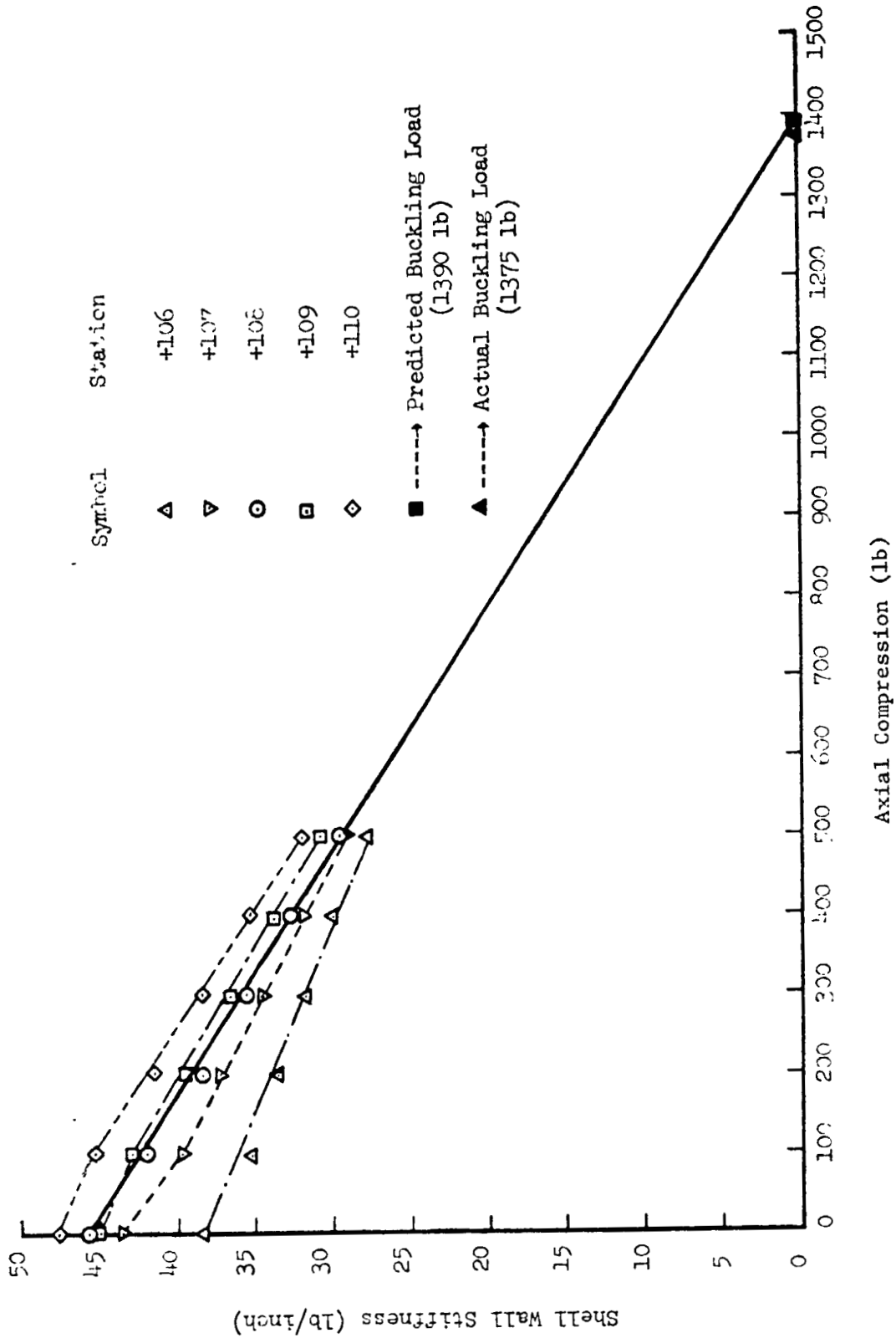


Figure 6. Stiffness-Axial Load Plots for Unstiffened Circular Shell.

Table II Stiffness Profile of Unstiffened Circular Shell Under Zero Axial Compression.

Generator	Normal Stiffness (lb/inch)												
	Distance of the Measurement Plane From the Equatorial Plane of the Shell												
	6"	5"	4"	3"	2"	1"	0"	-1"	-2"	-3"	-4"	-5"	-6"
1	65.3	67.8	65.6	58.6	52.5	53.8	44.1	43.4	48.0	53.1	54.7	63.7	64.5
2	72.0	52.8	63.1	50.4	42.1	45.7	44.8	40.7	47.3	47.9	51.9	53.4	67.0
3	65.4	52.6	56.0	48.0	41.0	45.4	43.6	39.6	46.3	49.7	52.1	52.0	66.4
4	71.0	50.8	56.0	43.1	41.7	45.5	42.6	38.5	48.7	45.7	47.1	50.0	62.1
5	68.4	43.5	48.4	40.6	39.8	45.5	42.6	40.8	47.2	45.1	46.2	48.7	61.8
6	69.9	48.8	47.7	41.6	38.2	40.7	40.6	37.7	41.8	42.5	45.4	47.5	61.6
7	74.2	49.2	45.5	40.6	37.6	39.8	37.8	37.8	40.8	40.3	45.6	46.5	57.3
8	63.0	48.8	49.7	41.6	37.9	40.6	37.5	38.3	38.5	41.8	43.1	46.2	59.5
9	74.9	47.1	43.8	40.7	37.7	46.2	35.7	37.5	39.1	40.0	41.2	45.8	66.7
10	67.0	51.3	38.8	41.0	36.8	45.0	39.1	37.6	40.4	43.3	41.8	46.8	63.3
11	69.7	47.6	44.2	38.2	37.8	43.2	41.6	40.3	43.6	48.2	44.9	49.6	54.4
12	69.4	49.7	49.0	47.8	40.4	46.2	43.2	42.3	42.5	48.2	48.0	53.2	61.8
13	78.7	52.5	47.4	45.0	43.1	47.4	46.1	45.3	43.0	42.8	48.3	52.1	61.2
14	77.5	54.8	54.6	44.8	43.9	51.8	47.1	41.7	47.8	47.7	51.3	52.3	63.9
15	66.8	61.6	58.9	51.5	42.7	53.2	44.7	47.1	48.2	53.0	53.5	52.4	62.2
16	64.5	53.8	49.3	50.2	44.8	56.1	48.7	45.1	47.5	52.0	56.0	56.8	63.0
17	63.0	61.4	63.0	48.4	44.5	49.3	50.1	48.6	46.7	48.3	58.2	55.1	63.4
18	72.4	63.4	61.6	52.7	49.1	52.2	52.8	55.8	47.4	51.4	60.1	54.2	66.4
19	75.4	72.2	74.0	55.1	49.6	58.2	55.6	56.6	47.1	91.1	62.1	62.9	72.7
20	70.0	65.6	71.7	68.7	55.3	62.6	59.4	55.0	52.0	54.5	56.0	58.8	74.6
21	76.6	69.5	80.4	67.5	54.2	66.6	60.3	60.7	52.4	56.8	62.3	59.2	80.6
22	96.0	71.9	81.0	71.2	57.5	79.3	65.5	61.2	52.4	61.0	68.6	59.5	78.7
23	130.6	78.5	88.6	70.2	61.2	82.1	69.8	71.8	57.5	58.5	69.4	65.4	83.4
24	145.9	88.5	77.3	76.5	58.8	78.5	80.5	80.8	72.8	67.1	67.5	77.8	89.9
25	111.1	83.6	83.4	93.5	64.2	75.5	69.2	76.3	70.7	67.3	73.4	70.4	77.7
26	173.9	77.4	92.8	73.0	63.3	78.2	81.2	78.0	70.3	66.9	75.4	67.4	84.4
27	114.8	74.3	98.2	86.0	75.2	77.3	78.1	74.9	74.6	70.4	69.0	67.2	86.1
28	110.0	102.0	98.1	76.8	69.9	74.0	86.7	73.4	72.9	75.3	68.4	69.1	89.1
29	98.8	80.5	106.4	70.2	62.9	65.6	78.8	65.1	67.8	69.3	63.9	69.7	92.3
30	104.1	88.3	90.6	67.5	58.6	61.9	68.7	61.9	59.7	63.7	65.4	70.1	82.1
31	91.2	112.4	77.3	68.2	56.8	62.7	69.4	68.4	68.2	62.3	57.5	70.3	84.4
32	100.4	83.7	100.9	106.4	63.1	106.0	80.9	80.2	83.9	100.9	89.8	76.8	132.3
33	103.7	105.8	76.4	84.1	76.1	81.2	78.7	79.7	87.1	84.9	101.5	77.2	118.8
34	110.1	107.3	101.4	98.5	64.3	73.2	57.3	67.9	75.9	79.9	80.5	71.1	91.5
35	117.0	78.1	85.5	62.0	47.5	52.7	52.6	46.8	57.0	48.6	60.1	58.6	74.2
36	.....	.....	.....	.....	.....	.....	.....	.....	.....	.....	.....	.....	.....

..... Seam of the Shell - Data not acquired.

#### 2.4 An Evaluation Method Based Upon the Variation of Dynamic Mass.

In the prior section a method of evaluation based on wall static stiffness was described and observations made relevant to the problems associated with its application. In this section a vibration method which to some degree reduces these difficulties is discussed.

The concept of static wall stiffness variation and the concept of dynamic mass variation are closely akin. Thus Nassar (14) undertook a study to determine whether or not the latter variation could be likewise used.

In view of the prior research on the association of vibrational behavior and instability (Discussed in more detail in Refs. 14 & 15) a column and a flat plate were included in the test program.

The shaker system consisted of a MB Vibramate Exciter (Model PM 25) driven through a MB power amplifier (Model 2125) by a PAR sinusoidal output oscillator (Model 110). This was mounted in such a manner as to ensure good positional control and to enable the shaker system to apply sufficient normal force preload to maintain contact with the specimen surface during the excitation cycle. The shaking force and the resulting acceleration were measured at the excitation point. The transducer was a BK Impedance Head (type 8001). The transducer output signals were conditioned with MB Line Drivers and MB N 400

signal amplifying units. The conditioned outputs were fed into a SD 101 B Dynamic Analyser/Tracking Filter of 1.5 Hz band width tuned to the excitation frequency. The final link in the data acquisition chain was a HP 2115 A computer and a HP 2402 A integrating digital voltmeter. These later elements were combined with a crossbar scanner to form the universal data acquisition and processing system used in the prior referenced tests.

It was found that the dynamic mass at any point was sensitive to the level of the excitation force used. However, for a fixed excitation frequency and a constant axial load the dynamic mass varied smoothly with the level of excitation force. Figures 7 & 8 show typical relationships between dynamic mass and average excitation force for various values of axial load. It is clear that each curve has a distinct minimum. When the minimum values of dynamic mass for a given frequency are plotted against the appropriate axial load level a linear relationship results, as shown in Figures 9 & 10. It is to be noted that this line intercepts the load axis at a point which is common for all frequencies and which corresponds to the critical axial load value.

A complete summary of the results obtained is presented in Table III.

It should be noted in connection with this method that the acquisition of data is a little easier than is the case with the



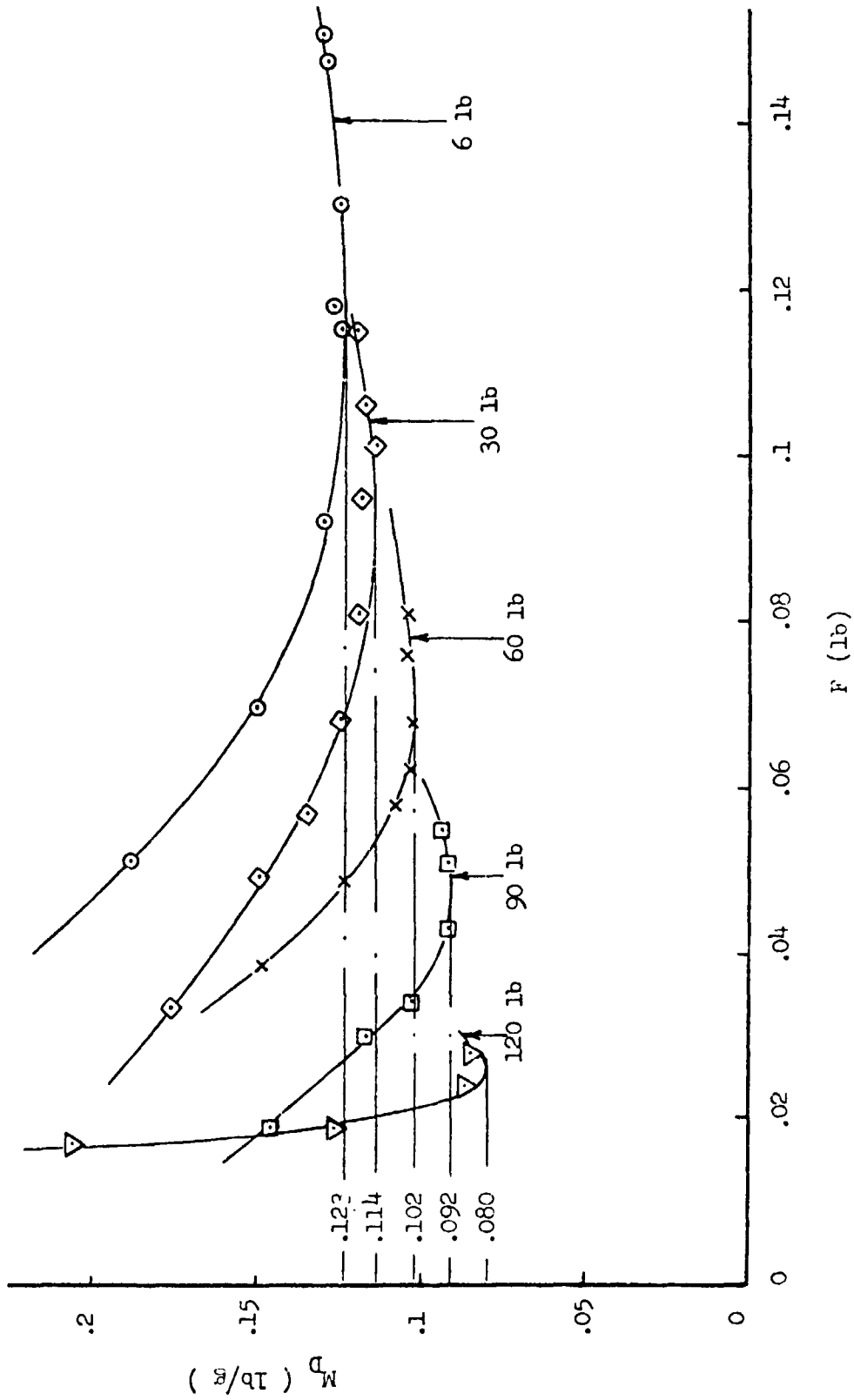


Figure 7. Elliptic Shell -  $M_D$  vs.  $F$  at 20 Hz.

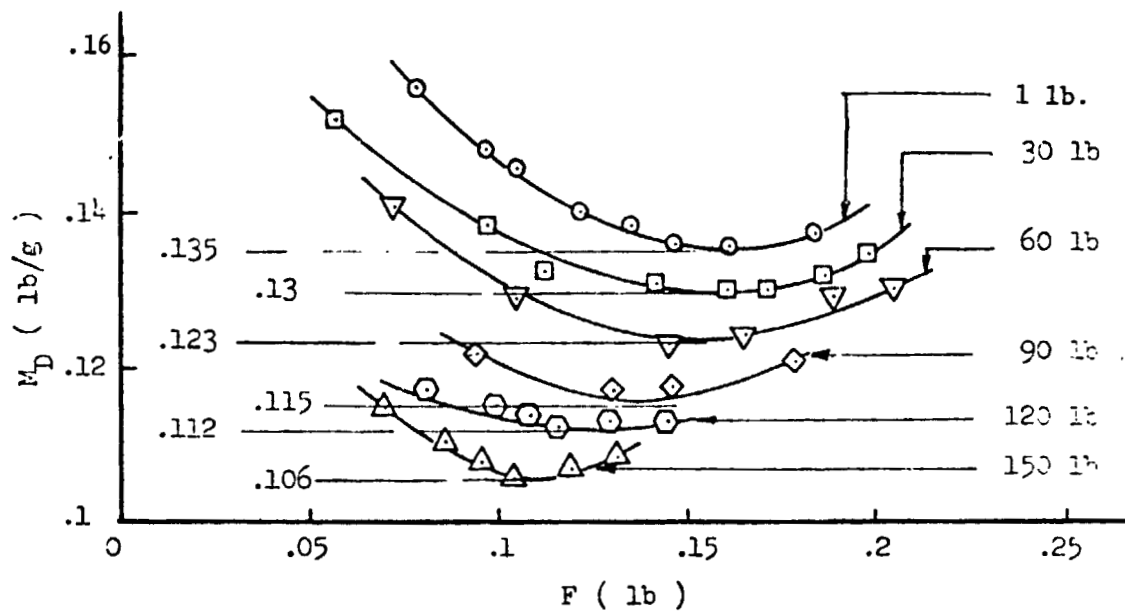


Figure 8. Rectangular Panel -  $M_D$  vs.  $F$  at 30 Hz.

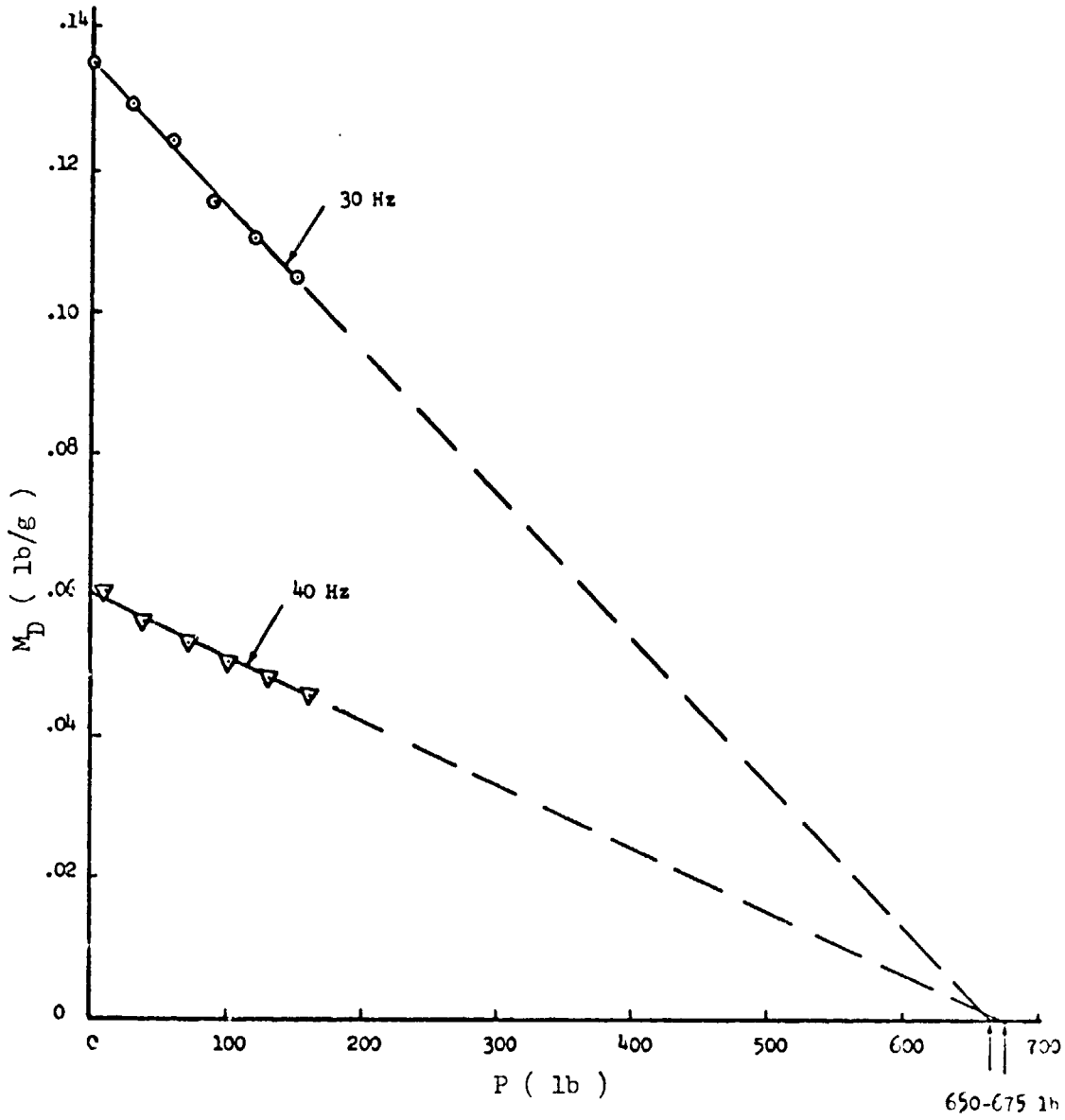


Figure 9. Rectangular Panel - Minimum  $M_D$  vs. Corresponding  $P$ .

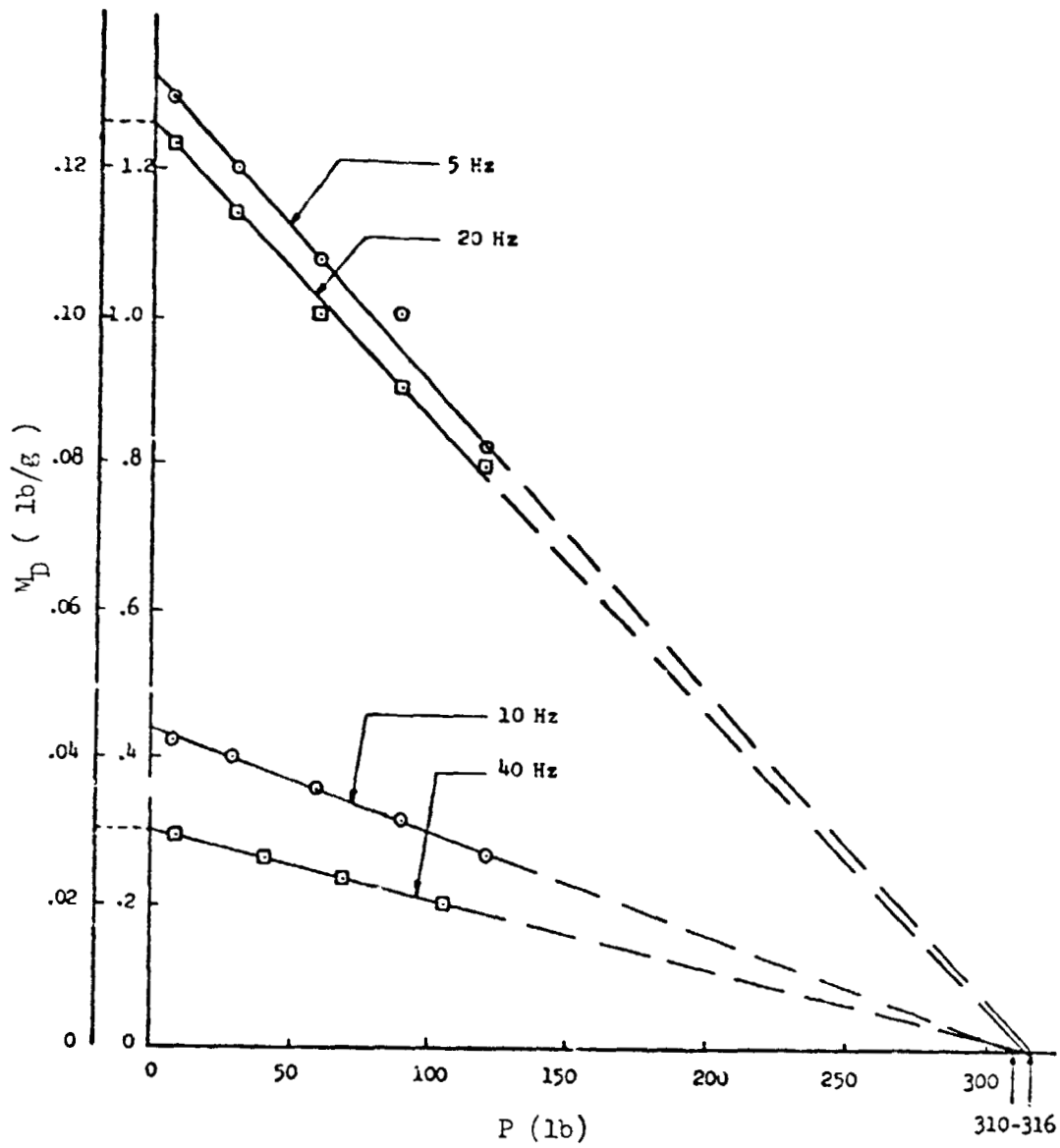


Figure 10. Elliptic Shell - Minimum  $M_D$  vs. Corresponding  $P$ .

Table III. Comparison of buckling loads predicted from dynamic mass variation with those achieved on test.

Specimen	Lowest Predicted Buckling Load (lb)	Actual Buckling Load (lb)	% Error	Remark
Column	6183	5872	+5.3	Actual buckling load was determined by Southwell Method.
Panel	2891	2958	-2.3	Actual buckling load was determined by Southwell Method.
Unstiffened Circular Shell	5049	5316	-5.0	Actual buckling load is the load at which snap occurred. (Buckled Elastically)
Unstiffened Elliptic Shell With A Rectangular Cutout	1379	1490	-7.5	Load offset to produce instability away from the cutaway region. Actual buckling load is the load at which snap occurred. (Buckled Elastically)

General Note: The shells used for the vibration study were the same as those for static stiffness study. The discrepancies in load carrying capability are due to variations in the applied loading distributions. The Southwell method was used for the column and plate to avoid ambiguity in definition of the actual buckling load.

wall stiffness method but the interpretation of the data is somewhat more involved.

### 2.5 An Evaluation Procedure Based on Combined Loading.

Duggan (16) and Craig and Duggan (17) investigated the issue from a somewhat different viewpoint. Circular cylindrical shells, both stiffened and unstiffened, under axial load are imperfection sensitive structures. Similar bodies, however, when loaded by forces normal to their surface are not. Such forces nevertheless are destabilizing.

Thus the above referenced investigators studied the behavior of a monocoque right circular cylindrical shell of 16" in length, 11.2" diameter and 0.030" wall thickness under the action of a point load normal to the shell wall and a uniform axial compression. They discovered that for fixed levels of axial load the normal force - wall deflection history was initially linear but subsequently became hyperbolic, (Figure 11). Data from this loading combination were analyzed, in the Southwell manner, for different levels of applied compression. The result was an interaction relationship which was essentially linear. Thus it was simple to extrapolate the curve of critical lateral force versus axial compressive load and so deduce the critical compressive load for zero lateral force. Their result is shown in Figure 12.

The general validity of their approach cannot be denied but it

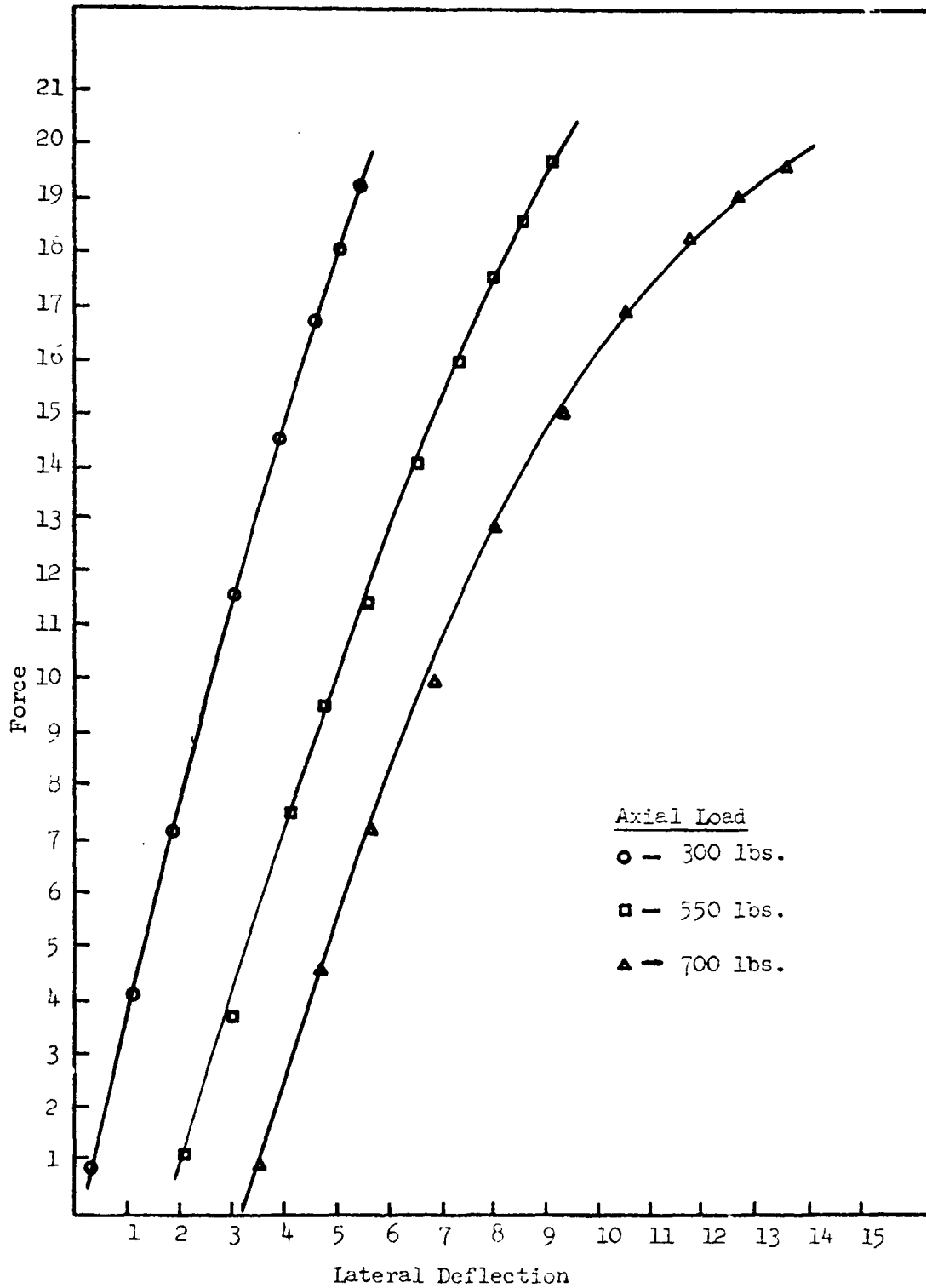


Figure 11. Load - Deflection Plots, Increasing Axial Load, for 220 Degree Angular Position.

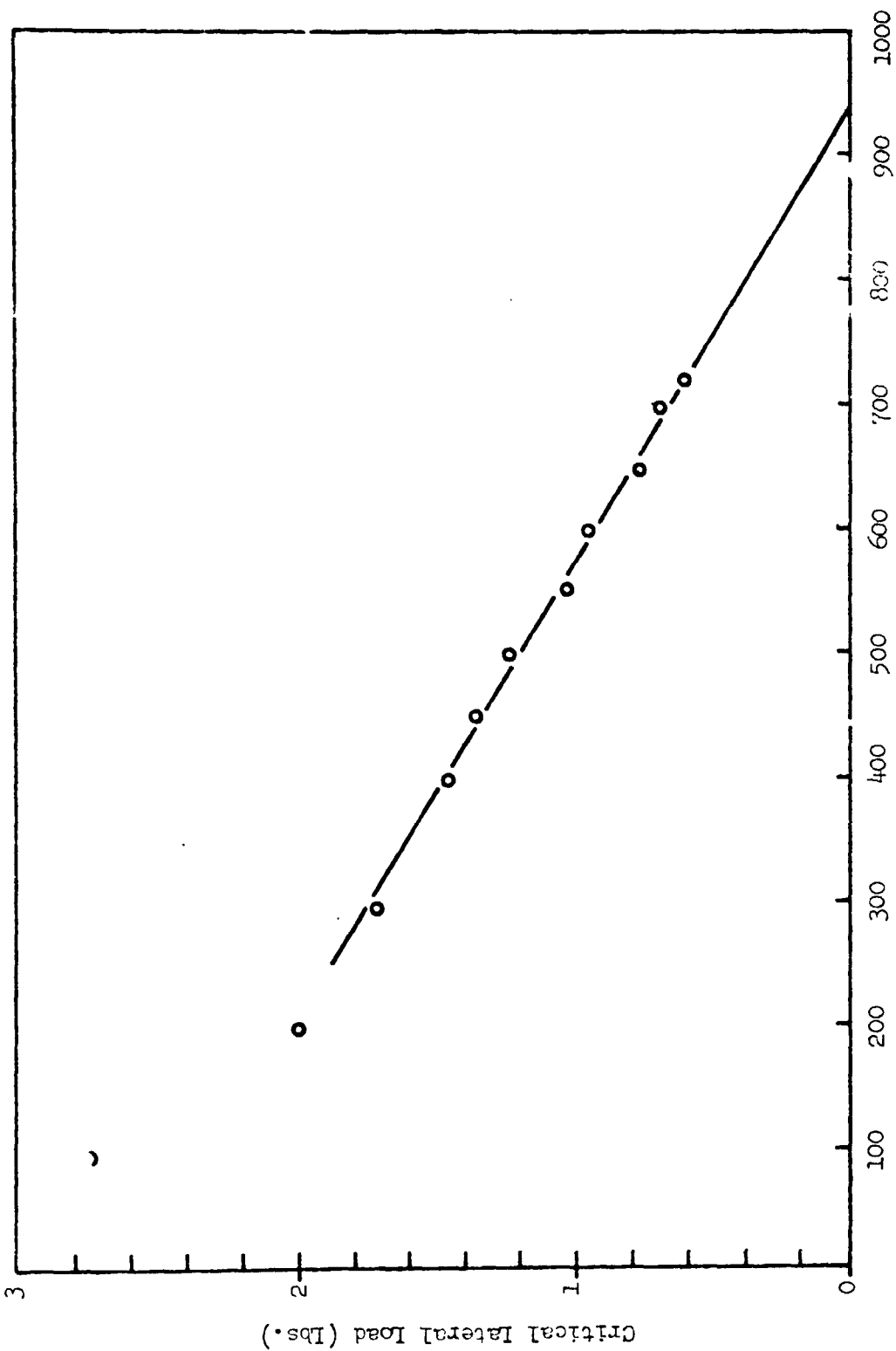


Figure 12. Critical Lateral Force Behavior Under Axial Compression.



must be pointed out that experimental confirmation was made on one shell only. Moreover, the approach is a little more time consuming than the direct stiffness approach because of the labor involved in computing the critical lateral forces from the displacement data.

#### 2.6 Conclusions Drawn From the Results of the Non-Destructive Evaluation Program.

It was concluded from the results, which are summarized in the previous sections that, unless the large scale vehicles have characteristics which seriously deviate from those of the models, it should be feasible at low levels of axial force to accurately determine the areas of weakness of the large shells and their probable critical loads. It was recognized, however, that some difficulties could be experienced because of the scale of the vehicle and in view of the difference in load application method.

#### 2.7 A Parametric Study on Ring Stiffened Shells.

The results which were generated in the study summarized in Section 2.1 led Ford (8) to make a parametric study on ring stiffened shells. To this end he investigated 6 different longitudinal stiffening arrangements and 41 different ring arrangements. The characteristics of the prime components of the shells which he used are summarized in Table IV and the results which he obtained are delineated in Tables V and VI.

TABLE IV CHARACTERISTICS OF THE FRAMES & STRINGERS OF THE SHELLS USED IN FORD'S PARAMETRIC STUDIES

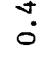
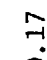


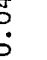
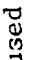

Shape	Stringer Type	Frame Type	Area ins <sup>2</sup>	Centroid Height	10 <sup>3</sup> . I ins. <sup>4</sup>	10 <sup>4</sup> . J ins. <sup>4</sup>	Shell Family
	A	A	0.063	0.125	0.325	0.46	0300 0400 0500
	B	not used	0.032	0.158	0.17	0.60	06XX
 n layers	not used	Bn	0.0075n	0.015n.	---	---	08XX 09XX 10XX
	C	C	0.033	0.123	0.13	0.28	0701
	D	not used	0.0404	0.110	0.20	0.74	08XX
	E	not used	0.0206	0.209	0.15	0.0517	09XX
	F	not used	0.0177	0.0742	0.078	0.038	10XX

Table V  
CHARACTERISTICS OF SHELLS WITH UNIFORM RIBS AND STRINGERS.

Shell Number	Nominal Diameter	Wall thickness	Length (in.)	Number of Frames	Frame Pitch (in.)	Frame Type	Number of Stringers	Stringer Pitch (in.)	Stringer Type	Computed Critical P <sub>cr</sub> (lb.)	Southwell Critical P <sub>sw</sub> (lb.)	Actual Critical P <sub>exp</sub> (lb.)	n <sub>cr</sub>	n <sub>exp</sub>	P <sub>sw</sub> /P <sub>cr</sub>	P <sub>exp</sub> /P <sub>cr</sub>	P <sub>exp</sub> /P <sub>sw</sub>
0300	↑	↑	13.25	3	C	A	47	1.00	A	16,049	-	14,650	-	-	-	0.91	-
0400	↑	↑	16.50	4	O	A	47	1.00	A	16,864	-	14,750	-	-	-	0.88	-
0500	↑	↑	19.75	5	N	A	47	1.00	A	16,792	-	15,200	-	-	-	0.92	-
0601	↑	↑	↑	4	F	B1	60	↑	B	3,084	5,700	5,290	6	7	1.84	1.73	0.93
0602	A	A	A	4	A	B2	63	N	B	5,183	7,500	-	5	6	1.45	-	-
0603	L	L	L	4	N	B3	61	I	B	7,852	8,300	-	5	5	1.05	-	-
0604	L	L	L	4	T	B4	61	F	B	10,000	11,650	-	5	5	1.16	-	-
0605	S	S	S	4	3.30	B5	61	O	B	13,238	13,700	-	5	5	1.03	-	-
0606	S	S	S	4	I	B6	61	R	B	15,857	15,200	-	5	4	0.96	-	-
0607	H	H	H	4	N	B7	61	M	B	18,711	17,250	-	4	4	0.93	-	-
0608	L	L	L	4	C	B8	61	L	B	21,212	17,200	-	4	3	0.80	-	-
0701	S	S	S	4	H	C	47	0.733	B	12,500	13,300	-	4	5	0.94	-	-
0800	W	W	W	4	S	-	47	1.030	C	2,150	3,900	-	6	7	1.82	-	-
0801	E	E	E	0	-	-	47	↑	D	2,537	4,000	-	6	7	1.58	-	-
0802	E	E	E	1	8.12	B1	47	N	D	2,902	4,100	-	6	7	1.41	-	-
0803	E	E	E	3	4.06	B1	47	I	D	3,579	4,330	-	6	7	1.14	-	-
0804	↑	↑	16.50	7	2.03	B1	47	F	D	5,943	6,000	-	6	7	1.01	-	-
0807	I	I	I	7	2.03	B2	47	O	D	8,901	8,230	-	5	5	0.93	-	-
0810	N	N	N	7	2.03	B3	47	R	D	11,999	11,300	-	5	5	0.95	-	-
0813	C	C	C	7	2.03	B4	47	M	D	9,463	9,060	8,100	5	5	0.96	0.86	0.89
0814	H	H	H	3	4.06	B4	47	L	D	3,188	4,870	-	6	6	1.53	-	-
0901	I	I	I	4	C	B1	72	1.021	E	5,188	6,430	-	5	6	1.24	-	-
0902	N	N	N	4	O	B2	72	↑	F	8,204	8,850	-	5	6	1.08	-	-
0903	D	D	D	4	N	B3	72	N	E	10,814	12,000	-	5	6	1.11	-	-
0904	T	T	T	4	A	B4	72	F	E	14,009	13,700	-	5	6	0.97	-	-
0909	A	A	A	4	R	B5	72	O	E	17,200	14,800	11,900	4	3	0.86	0.70	0.81
0911	E	E	E	4	3.30	B6	72	R	E	1,863	4,100	3,720	7	7	2.20	2.00	0.91
1001	↑	↑	↑	0	↑	-	72	0.650	F	3,512	4,600	4,130	7	7	1.31	1.38	0.96
1002	↑	↑	↑	1	8.12	B2	72	↑	F	4,452	5,430	5,160	7	7	1.22	1.16	0.95
1003	↑	↑	↑	3	4.06	B2	72	↑	F	-	-	-	-	-	-	-	-

Table VI

CHARACTERISTICS OF SHELLS WITH NON-UNIFORM RINGS AND UNIFORM STRINGERS

Shell Number	Number of Frames	Pitch (in.)	Frame Number (1-7) and Type							Number of Stringers	Stringer Pitch (in.)	Type	Southwell P SW (lb)
			1	2	3	4	5	6	7				
0804	7	2.03	B1	B1	B1	B2	B1	B1	B1	47	1.021	D	5230
0806	7	2.03	B1	B2	B1	B2	B1	B1	B2	47	1.021	D	5330
0808	7	2.03	B2	B2	B2	B3	B2	B2	B2	47	1.021	D	7900
0809	7	2.03	B2	B3	B2	B3	B2	B2	B3	47	1.021	D	8000
0811	7	2.03	B3	B3	B3	B4	B3	B3	D3	47	1.021	D	9150
0812	7	2.03	D3	B4	B3	B4	B4	B3	B4	47	1.021	D	9240
0902	4	3.30	B1	B2	B2	B1	B1	-	-	72	0.650	E	6440
0904	4	3.30	B3	B2	B2	B3	B3	-	-	72	0.650	E	7000
0906	4	3.30	B5	B4	B4	B3	B3	-	-	72	0.650	E	10200
0908	4	3.30	B6	B5	B4	B5	B5	-	-	72	0.650	E	11400
0910	4	3.30	B6	B5	B5	B6	B6	-	-	72	0.650	E	13600
1008	3	4.06	B3	B2	B3	-	-	-	-	72	0.650	F	6360*

General Note: All shells had a nominal diameter of 15.0 in., a wall thickness of 0.030 in. and were 16.5 in. in length. All frames were external and of the layered variety.

\* Actual instability load established by test 5750 lb.

For a particular longitudinal stiffening the various types of external multilayer ring stiffened shells were made by successive modification of one basic shell. This was simply done since the individual layers of which the rings were made were very flexible. The added layers were glued to the prior layers by capillary gluing. One very great advantage of this method was that the process could be carried out with the specimen installed in the test machine. Thus, the distribution of line load for each shell of a family was substantially the same as that for all other members of the family.

The results for all rings of equal stiffness offer no surprises. They do, however, demonstrate conclusively that end restraint effects are of considerable importance in longitudinally stiffened shells which have relatively light ring stiffening, and thus completely support the work of Peterson (18).

Perhaps the most interesting quantitative data acquired is that relative to instability behavior when all rings do not have equal stiffness. These results are portrayed graphically in Figures 13 & 14.

Ford also points out in his thesis that both longitudinal and circumferential waves appear in the pre-buckling deformations of axially compressed, imperfect stiffened shells. This observation is in full agreement with those reported in References 19, 20 and 21. He notes also that these pre-buckle deformations are such as to

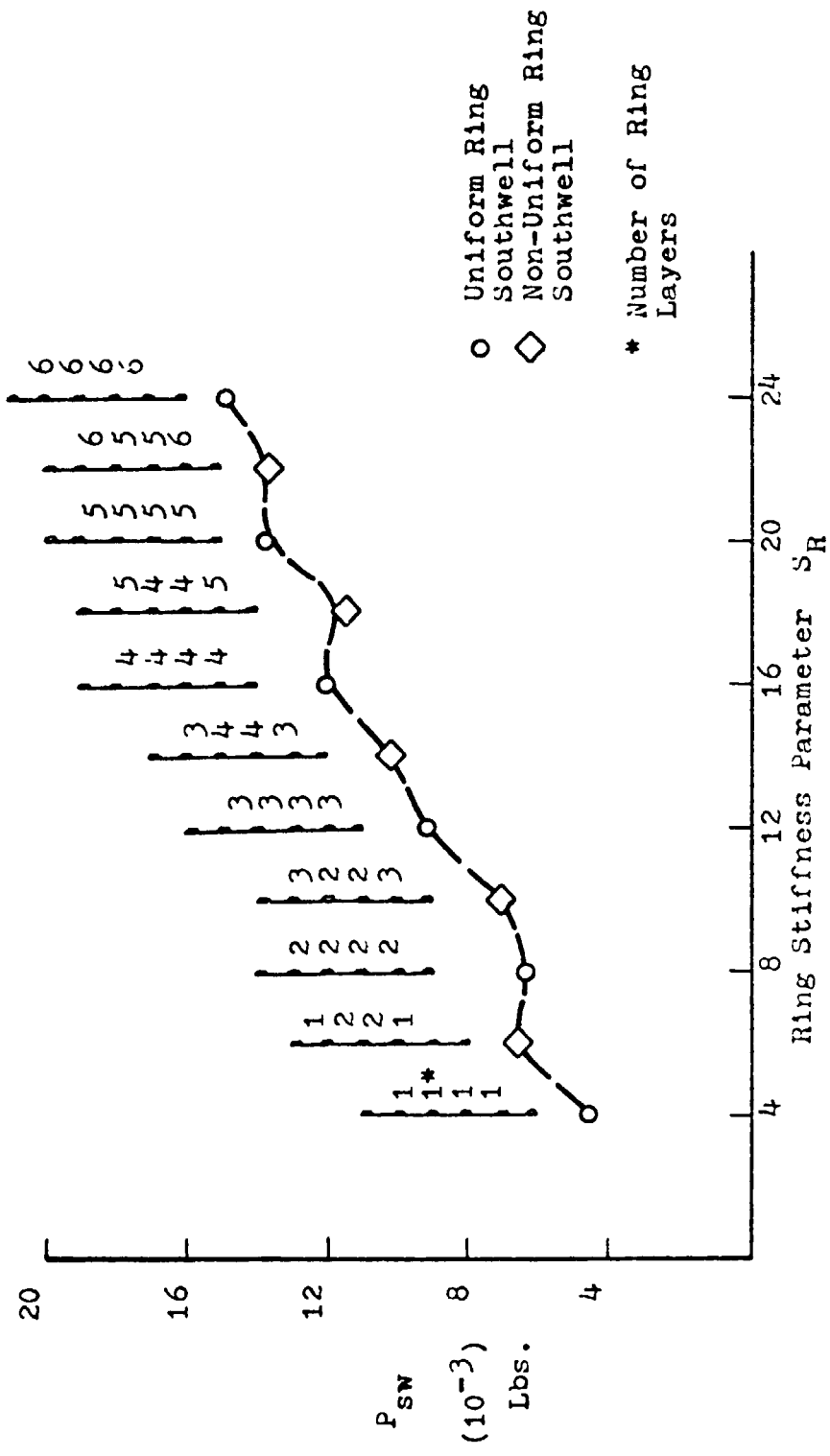


Figure 13.  $P_{SW}$  versus  $S_R$  • Non-Uniform Rings, Shell 09XX.



validate the choice of basic displacement function made in the linear theory development (22)

### 3. Tests on Large Scale Stringer and Ring Stiffened Shells.

#### 3.1 General Remarks.

As noted in the introductory remarks the prime purpose of the program reported here was the study of large scale, realistically reinforced circular cylindrical shells liable to general instability. It was the intent to acquire shells of high quality and to test these under as uniform distribution of axial load as could be attained. To meet these definite objectives special shells were designed at the Georgia Institute of Technology and manufactured by Skinner Aviation, Miami, Florida. These shells were tested in a facility specifically constructed for the purpose. In the sections which follow details of the shells, the method of preparation for test, the test facility, the instrumentation and the major results are outlined.

#### 3.2 Details of the Shells.

##### 3.2.1. Main Body Construction.

All the shells used in this program were made of aluminum alloy (Spec. 7075-T6) and had identical overall dimensions. They were 74.5 inches in diameter and 108 inches long. Each shell was made from 6 identical panels. These panels had a nominal skin thickness of 0.0253 inches and were reinforced



by a multiplicity of Z-shaped stringers which had the cross-sectional shape shown in Figure 15. One edge of each panel was joggled, and two stringers were riveted along each joint line with 0.125 inch diameter rivets at 0.75 inch pitch. The remaining stringers were attached to the sheet with adhesive FM 126-2.

The ends of the shells were reinforced with a 0.040 inch thick doubler plate of 7075-T6 material. They were held circular by means of heavy rolled C section frames. These frames had the cross-section depicted in Figure 16. They were located in such fashion that 0.125" of reinforced shell wall protruded beyond their extreme face at each end of the shell.

The intermediate frames were rolled from the stringer section. They were attached either to the outer skin with rivets, whose pitch was identical to the stringer pitch, or to the lip flanges of the longitudinal stiffeners. In all cases in which the internal frames were used anti-peel rivets were driven in the skin and stringer base adjacent to the internal ring.

### 3.2.2. Main Body Inspection.

All the test vehicles were thoroughly inspected before test. In every case the bonded joints appeared to be of good

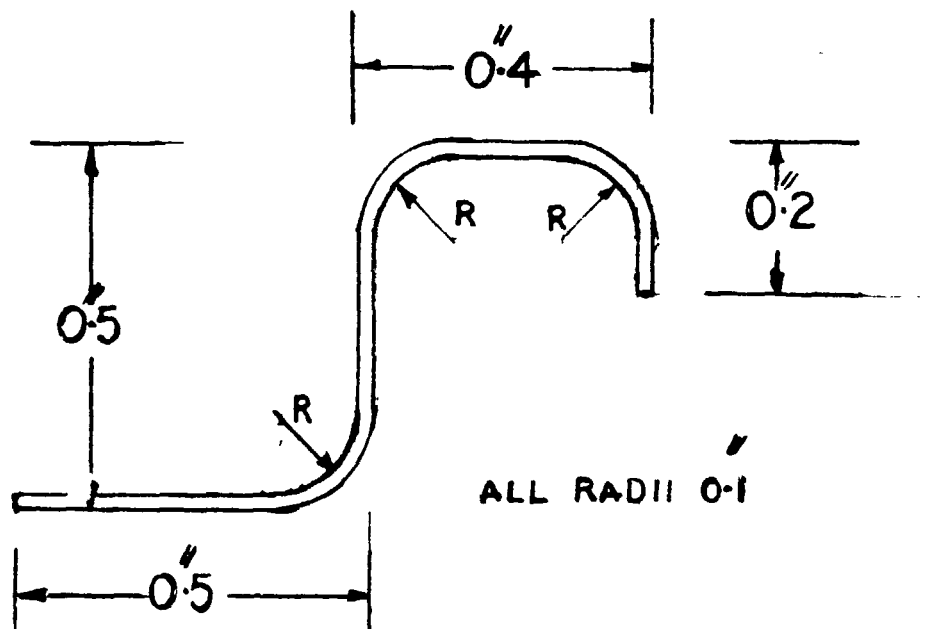


Figure 15. Ring and Stringer Section.

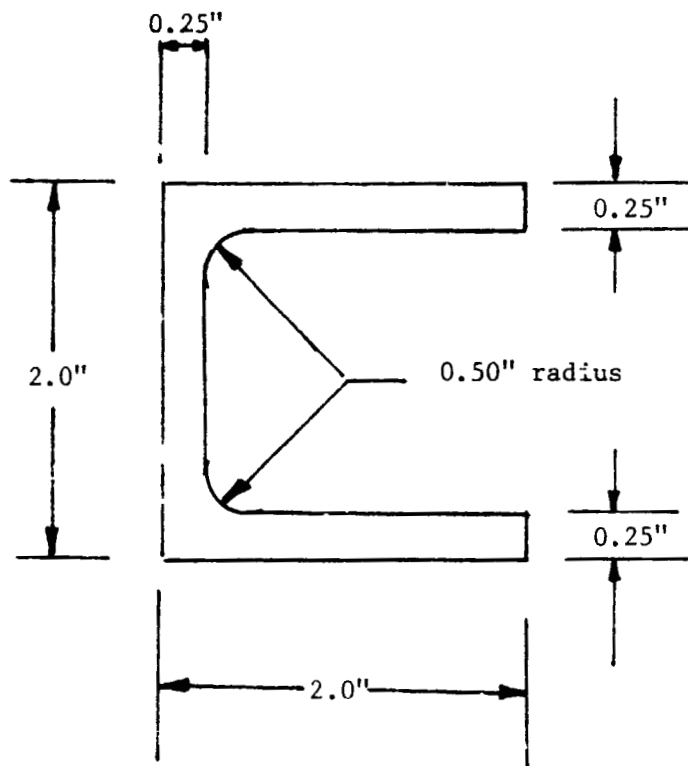


Figure 16. End Ring Section

quality. Test coupon joints made at the time of fabrication and using the identical process were always fully consistent and satisfactory. All riveted seams and joints were well made and tight.

Circularity and generator straightness was checked on all specimens, but a detailed study was made on two only. For this purpose stiff end plates, with central bearings, were attached to the specimen. The specimen was then mounted, with its axis horizontal, in a heavy framework in such fashion that it could be rotated about its axis. The shell was rotated about this axis and the variation of profile recorded at intervals along the length of the shell. A single linear variable differential transformer was used as the displacement transducer for all displacement measurements. To establish a known measurement reference, a ten foot precision straight edge was positioned outside the shell and parallel to the axis. The LVDT was then attached to the straight edge in such a manner that it could be positioned along the specimen axis as desired. An electro-optical system was used to transduce the angular position. A block diagram of the overall system is given in Figure 17. The method of analysis of the data acquired is given in Reference 16 and Reference 24. Computer programs pertinent to the analysis are likewise given in these documents.

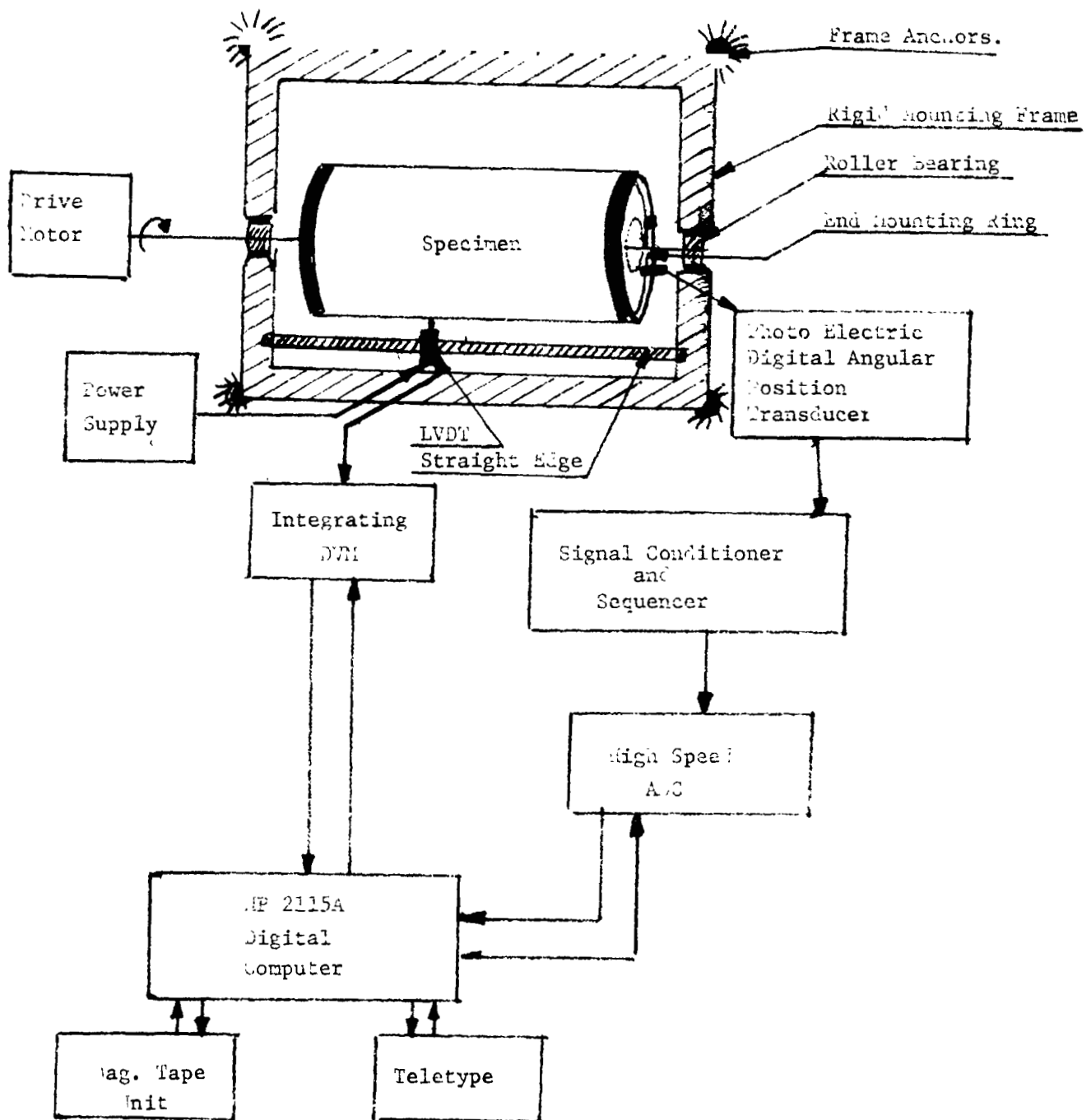


Figure 17. Block Diagram of Circularity Checking System.

### 3.2.3. Shell End Machining.

The desired uniformity of line load around the shell ends cannot be achieved unless a virtually perfect mating between the shell ends and the loading plates can be assured. A major issue was therefore to devise means of accomplishing this. To meet the objective a special machine was designed. (This is fully described in Reference 7). However, no machine can be made to perform the task of trimming the ends flat unless the free extremities of the many stringers are thoroughly stabilized. This was done in two ways: 1) by setting the stringer ends in a matrix of low melting point alloy and 2) by setting the stringer ends in a matrix of automobile body putty.

The latter approach turned out to be by far the most economical and satisfactory. With the automobile putty the cutting tool remained sharp throughout the operation.

### 3.3. Test Facility.

The shells were tested in the School of Aerospace Cylindrical Shell test facility, which is described in detail in Reference 23.

The structural test complex has two main components, 1) the loading and force reaction system and 2) the data acquisition and processing system.

### 3.3.1. The Loading and Force Reaction System.

The basic principle of the loading and force reaction system is illustrated in Figure 18. The compressive load was applied by a multiplicity of hydraulic actuators positioned around the base of the shell. For one shell (shell B) 72 actuators, Enerpac RC 1010, were used. For the other shells 18, OTC No. YS Shorty Type, were employed. The actuators were attached to a heavy retainer ring via radially adjustable base plates. They were arranged so that their centers of thrust lie on a circle whose diameter matched that of the centroidal locus of the shell under investigation.

The force provided by the jacks was fed into the test structure via a bearing plate or structure. (The bearing plate was used with the 72 jacks and the bearing structure with the 18 jacks). Under no load conditions the bearing devices were carried on adjustable supports. These were so trimmed that the upper bearing surface lie in a horizontal plane while the lower surface cleared the jack pads. Ball joints were provided between the jack heads and pads. (See Detail B.)

Load reaction was via a special upper reaction ring which was tied to the jack support ring by 36-1" diameter steel

REPRODUCIBILITY OF THE ORIGINAL PAGE IS POOR

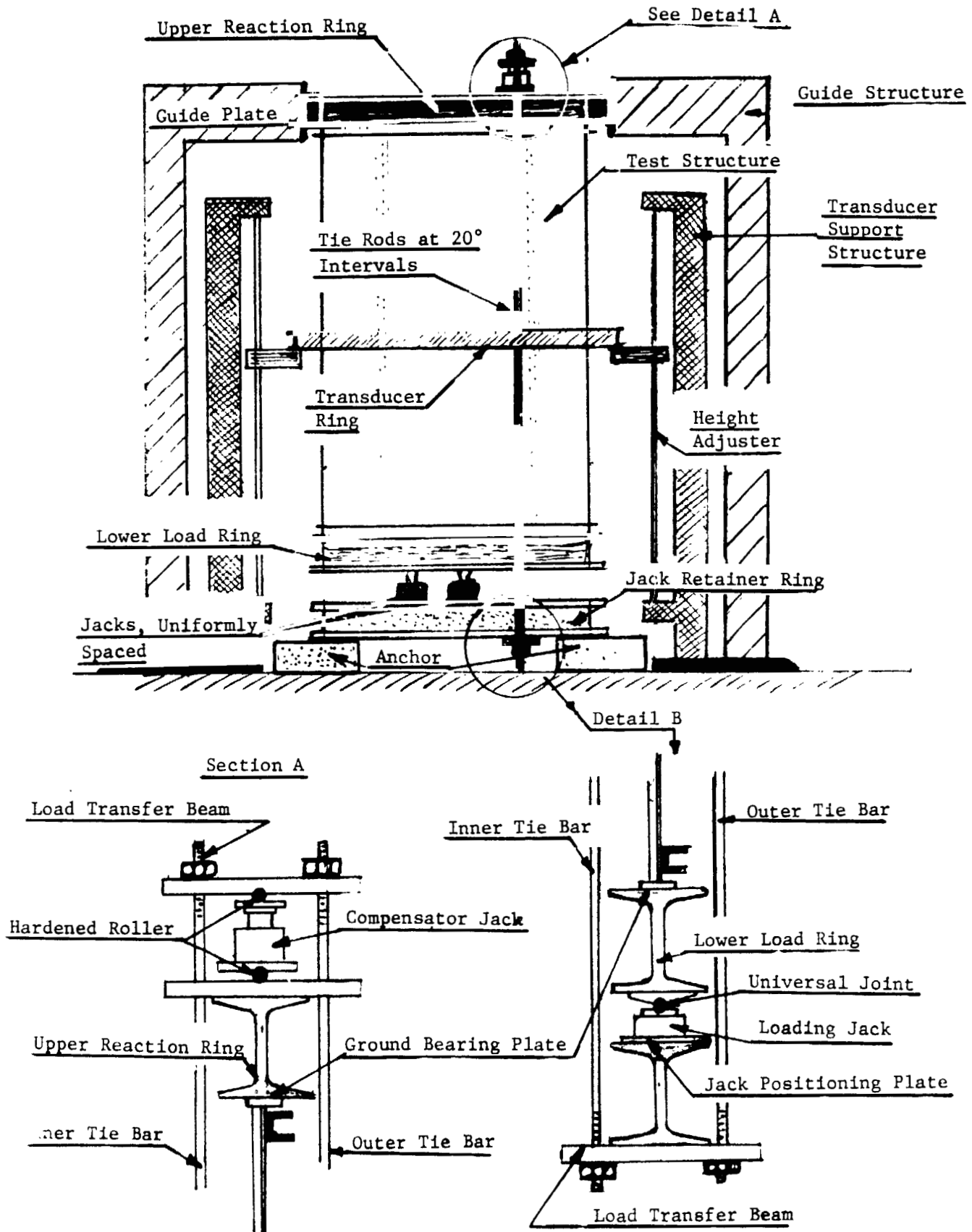


Figure 18. Schematic of Large Shell Testing System



tie bars. A direct tie bar system would give rise to considerable trim difficulties and so high quality hydraulic load cells were fitted between the tie rod transfer beams and the upper surface of the reaction ring, Detail A. These reaction cells were interconnected to form a closed system.

### 3.3.2. Hydraulic System.

The hydraulic power for the load actuators was provided and controlled via a servo-control system of orthodox character. All load jacks were interconnected and fed from this common source.

### 3.3.3. Load Determination.

Load was determined from the pressure applied to the loading actuators. The pressure generated in the reaction cells was used as a check. These hydraulic pressures were read on precision pressure gauges manufactured by Heise.

### 3.4. The Data Acquisition and Processing System.

The data acquisition and processing system used in the study was the Aerospace Structures Laboratory facility. The essential elements of this system are delineated in Section 2.1 and a data acquisition flow diagram is presented in Figure 1. (For more specific details see Reference 23).

### 3.5. Installation of the Test Vehicle in the Facility.

The test vehicle was installed in the following manner:

- (1) The lower jacks were accurately set in a circle of appropriate diameter.
- (2) The shell was hoisted into the rig and suspended above the jack system.
- (3) The lower load transfer structure was slid into position and the bearing pad aligned with the loading jacks.
- (4) The shell alignment guides were attached to the load transfer ring.
- (5) The shell was lowered into position.
- (6) The reaction pad, with upper load cells attached, was placed in position and aligned.
- (7) The tie-rods and bridging structures were placed in position.
- (8) The tie-rods were set vertical.
- (9) The reaction ring guide system was installed.
- (10) When the appropriate positions of all elements had been established, the mating of the load and reaction plates with the ends of the shell was investigated. This was done by separating the surfaces (\*a) and installing plastigages (\*b)

between them at closely spaced intervals. The mating surfaces were then brought into contact and a small axial force applied. After this slight compression the surfaces were again separated and the quality of fit determined from the degree of flattening of the gages. Except in the development of the machining process it was not found necessary to remove the specimen and make any changes as the result of this check. In all cases the gap between the mating surfaces was considerably less than 0.001 inches and this misfit was over very small localized areas.

- (11) In some cases a thin layer of Devcon, a viscous steel-filled epoxy, was spread between the mating surfaces. The mating surfaces were then squeezed together with a substantial compression. (\*c)

Special Notes

- (\*a) Due to the fact that it was necessary to stabilize the free ends of the stringers prior to end trimming, and the fact that this material was not removed after this operation was complete, plane surfaces existed at the ends of the shells.
- (\*b) Plastigages are small diameter rods of special plastic material. They are commonly employed for determination

of shaft-bearing slop, etc. They are made by Perfect Circle, Hagerstown, Indiana.

(\*c) Despite the liberal use of the appropriate parting compound, some Devcon became attached to the bearing plates. In view of the time and expense involved in restoring these surfaces to their original pristine condition, and the very slight improvement in distribution resulting from its use, the practice was discontinued. Devcon is a product of the Devcon Corporation, Danvers, Massachusetts.

### 3.6 Quality and Accuracy Achieved in the Large Scale Shell Program.

Every effort was made to attain the highest quality and accuracy throughout all phases of the work. The following sections summarize the results achieved.

#### 3.6.1. Shell Circularity.

The checks on circularity showed that the shells did not deviate appreciably from circular. The maximum amplitudes of the excursions were of the order 0.1 inch, see Figure 19 which presents typical data.

Detailed analysis indicated that:

- (1) There was a tendency towards ovality.
- (2) The lap joints kept the generators, in their immediate vicinity, very straight.

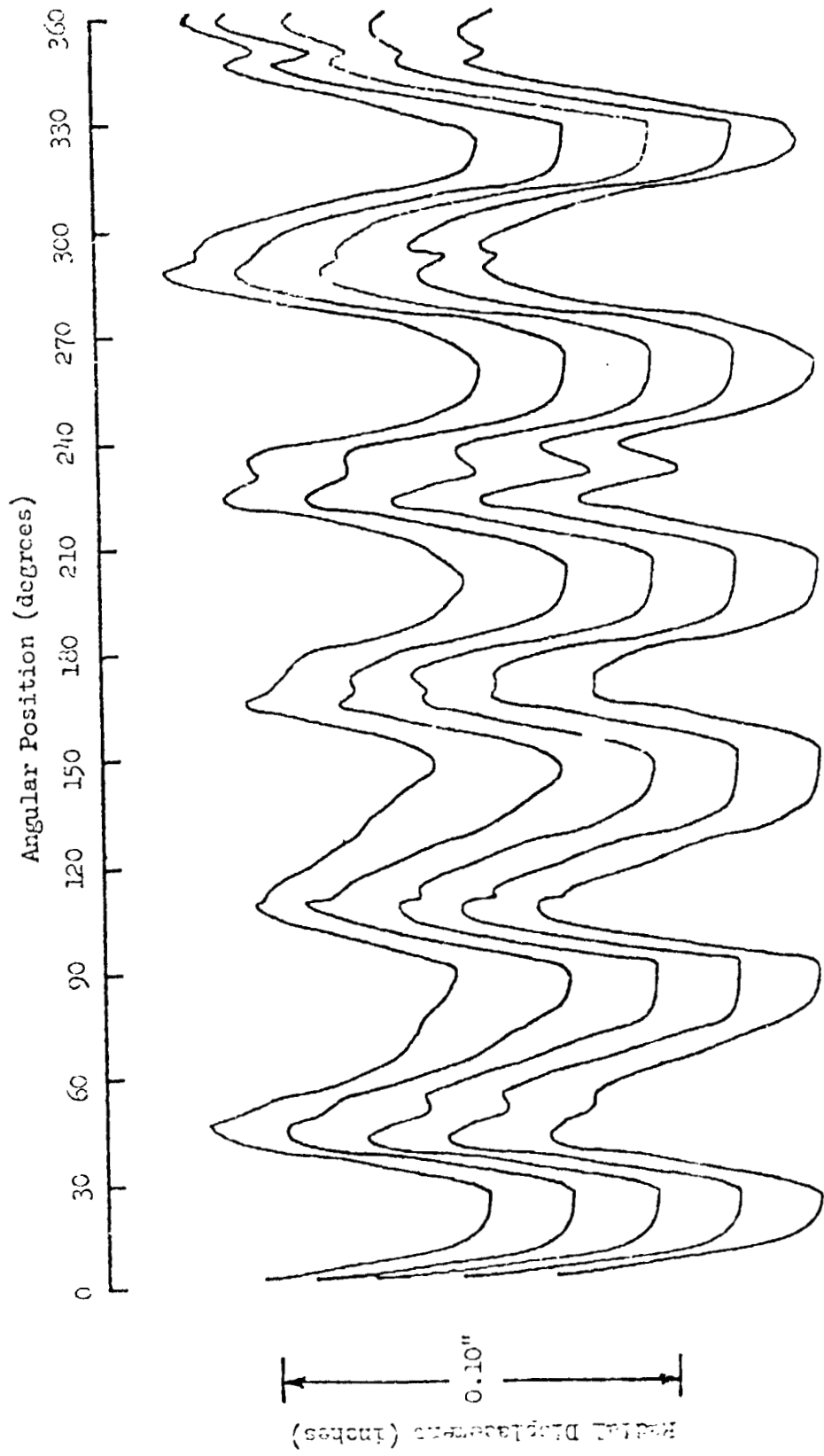


Figure 19. Large Shell Initial Geometry

(3) The lap joints had a significant influence on the circumferential deviations.

(4) The rings had little influence on the longitudinal deviations.

These later points are made clear by the data which is given in Tables VII & VIII,

#### 3.6.2. Shell End Quality.

The shell ends were parallel to within  $\pm 0.1^\circ$ , and local variations in flatness were controlled to within  $\pm 0.0005$  inch.

#### 3.6.3. Load and Reaction Bearing Surface Quality.

The load and reaction bearing surfaces were ground flat to within  $\pm 0.0005$  inch.

#### 3.6.4. Fit of Shell Ends on the Load and Reaction Bearing Surfaces.

Checks with plastigages showed that the maximum gap between the two surfaces - shell and bearing - was no more than 0.001 inch. Such variations were few in number and were local.

#### 3.6.5. Load Steadiness.

The servo control held the applied load so steady that no movement of the Heise pressure gauge needle was discernible.

Table VII

FOURIER SERIES COEFFICIENTS FOR DEVIATION DATA (CIRCUMFERENTIAL)

No of Waves	Amplitude in mils at stated distance from end									
	4".0	17".5	31".0	38".5	44".5	50".5	58".0	71".5	85".0	97".0
0	-30.5	-23.9	-11.6	-8.6	-6.4	.6	5.1	17.7	22.5	15.7
1	4.4	.9	2.7	3.6	4.1	4.0	4.3	2.9	1.3	5.0
2	55.9	56.6	56.1	56.0	56.5	57.0	56.8	56.8	56.6	56.1
3	5.8	9.5	12.1	13.2	13.9	14.9	15.9	17.6	17.1	15.9
4	1.9	.9	2.8	4.6	5.2	5.6	6.3	6.9	5.8	3.0
5	2.5	3.2	3.8	3.5	3.0	3.0	2.8	2.2	.6	1.2
6	6.4	11.9	11.1	10.1	10.2	10.2	11.0	14.6	12.2	6.9
7	.8	2.1	1.5	1.7	2.1	2.5	2.8	2.7	2.7	1.1
8	1.8	3.0	2.4	2.4	2.3	2.8	3.0	2.0	1.6	1.6
9	1.5	4.6	4.7	3.2	1.5	1.0	1.8	2.3	1.4	.7
10	1.7	2.5	3.8	2.8	1.7	2.3	4.5	5.0	2.2	.7

Table VIII

FOURIER SERIES COEFFICIENTS FOR DEVIATION DATA (LONGITUDINAL)

No of Waves	Amplitude in mls at stated number of degrees							
	9	53	99	143	189	233	279	323
0	19.5	-18.5	-38.9	32.0	44.7	-38.5	-40.6	51.2
1	23.1	40.0	15.8	8.1	33.2	32.6	10.8	28.9
2	11.0	16.3	10.8	6.9	14.3	15.3	6.9	9.8
3	7.0	12.0	4.9	3.7	8.3	10.5	3.2	3.9
4	4.9	6.9	2.5	0.9	5.2	6.0	2.1	3.4
5	3.8	5.6	2.2	1.2	4.7	4.8	2.1	2.8
6	3.5	5.1	2.1	0.9	4.2	4.4	1.7	2.6
7	3.8	4.8	2.7	2.1	4.0	4.5	2.2	2.6
8	3.3	4.3	2.4	1.7	3.5	4.1	2.3	2.6
9	2.8	3.5	1.5	0.9	2.9	3.4	1.3	2.1
10	2.5	3.3	1.6	1.2	2.9	3.3	1.6	2.1



#### 3.6.6. Repeatability.

The total system, load and instrumentation, gave excellent repeatability. The strain readings obtained for nominally identical loadings showed no significant variations.

#### 3.7. Results Obtained.

The results which were obtained in the tests made on four large shells whose characteristics are given in Table IX, are summarized in the sections which follow.

##### 3.7.1. Non-Destructive Evaluation.

The non-destructive evaluation methods which were devised on the model shells were not successfully applied to all large scale shells. The prime reason for this lay in the incompatibility of the test system for the large shells and the probing systems. It is clear from the earlier section (3.3.1) that the test arrangements for the large shells were such that there were, of necessity, considerable encumbrances around the outside of the shell. Their presence made the application of the dynamic mass method unworkable. There was insufficient room to use the extender system in an adequate fashion. These encumbrances likewise restricted the full operation of the wall static stiffness method. For the static stiffness technique the probe was much smaller than the extender, but the transducer ring was too flexible. Thus, the displacements which were caused by the applied normal force could

TABLE IX. GEOMETRIC CHARACTERISTIC OF LARGE SHELLS TESTED

SHELL	No. of Bays	Ring Location	Ring Pitch (in.)	No. of Stringers	Stringer Pitch (in.)	Shell Length (in.)	Shell Diameter (in.)	Nominal Wall Thickness (in.)	Nominal Stringer Area (in. <sup>2</sup> )	Nominal Skin Area (in. <sup>2</sup> )
A	9	Outside	12.0	234	1.00	108	74.5	0.0253	8.171	6.111
B	9	Inside	12.0	234	1.00	108	74.5	0.0253	8.171	6.111
C	8	Outside	13.5	312	0.75	108	74.5	0.0253	10.895	6.073
D	8	Inside	13.5	312	0.75	108	74.5	0.0253	10.895	6.073

not be measured, it was thought, with instruments mounted outside the shell. Wall motions therefore had to be determined using transducers which were internally mounted and this led, naturally, to such a time consuming process as to be impractical.

It was not until the end of last test was reached that methods of overcoming the difficulties were devised. At this late stage it was recognized that the tie rods, being under substantial tension, could well be used as the displacement transducer supports. A very simple device based on this concept was constructed and used at station 220°, Bay 5, shell A. The relative stiffnesses of the shell wall were ascertained for a side push of the order of 25 lb., for axial loads corresponding to jack pressures of 800, 1000, 1200 and 1400 psi. It was found that these stiffnesses decreased linearly with applied load. When the stiffness versus applied pressure curve was extrapolated the indicated critical pressure was 2170 psi. This was in excess of the actual value of 2000 psi but was in excellent accord with the 2195 psi value computed from the local strains.

The second method which was devised, at this time, was the use of self adhesive strain gauges of the Hickson variety. These gauges were installed back to back on the skin and the stringer lip. These devices likewise led to linearly varying stiffness parameter versus applied pressure lines. Several stations on the shell were checked in this manner and

the lowest critical pressure determined by this means was 1995 psi. This value is almost identical with the actual value of 2000 psi. There are two reasons why this result may be somewhat fortuitous. First, the Hickson gauges have a tendency to drift. Second, in order to install the inner gauges it was necessary to construct "mounting bases" by bridging three adjacent stringers with a tightly stretched thin sheet of aluminum foil. This foil was bonded to each stringer lip.

#### 3.7.2. Maximum Load Levels Attained.

The maximum loads which the shells carried are delineated in Table X .

#### 3.7.3. Buckling Behavior and Post Buckled Condition.

The shells all buckled in a characteristic diamond pattern and in the normal snap fashion. There was, however, a difference between the behavior of the shells with external rings and those with internal rings.. For the shells which had external rings the buckle pattern covered the complete surface. For the shells with internal rings this was not the case.

After removal of load the wide spread pattern on the externally ring stiffened shells was still evident throughout the structure. Rings were distorted from circles into somewhat flat sided figures. The extent of the flatness depending

Table X      CRITICAL LOADS AND STRESSES

Shell	Critical Load (lb.)	Critical Stress (lb./in. <sup>2</sup> )	Remarks
A	233,705	16,363	Buckle pattern completely covered shell. Rings remained distorted after removal of load. No sharp creases in skin.
B	284,281	19,905	Buckle pattern did not cover whole shell. After removal of load 50% shell undamaged. Frame torn, sharp creases and tear in other section.
C	255,907	15,081	See A
D	309,659	18,250	See B

somewhat upon the axial location. There were, however, no element failures of other than an instability type. No evidence that the shells or any part thereof had come into contact with the tie rods during the buckling process existed.

The shells with internal rings did not buckle in the same manner. For these shells the buckle pattern did not completely fill the shell surface. Moreover, in these cases, when the load was removed there was no visible signs of damage on at least one half of the surface. In those regions which were damaged there was strong evidence that the structure had violently come into contact with the tie bars during the instability. Frames were torn apart at their joints; there were very sharp creases in the skin and some local tearing.

#### 3.7.4. Load-Strain Relationship.

Strains were measured at 180 points. Ninety of the measuring stations were on the outer skin and 90 on the stringer lips. The longitudinal gauge stations were at the meets of 5 planes, normal to the shell generators, with the outer skin and the stringer lips. Circumferentially gauge stations were 20° apart and back to back. The vertical locations are given in Table XI.

The strain gages used were of the Micro-Measurement type, CEA-15-250 UW 120. They were installed in accordance

TABLE XI.      HEIGHT OF STRAIN MEASUREMENT PLANES ABOVE BASE PLANE

SHELL	Station 1	Station 2	Station 3	Station 4	Station 5
A	4.5	18	54	90	103.5
B	4.5	18	54	90	103.5
C	4.5	18	47.25	90	103.5
D	4.5	18	47.25	90	103.5

The units in above table are inches above base plane.

with the makers recommended procedures and their output was processed by the instrumentation system previously referenced.

Tables XII through XV are typical data print outs. Each table contains the full 180 channels of information for a specific applied load. In order to cover the whole family of shells tested one table is given for each of the four shells. The broad spectrum of loading is represented since each set of data corresponds to a different percentage of the appropriate critical load.

The strain data which was recorded shows that all shells behaved in a similar fashion in so far that -

- (1) In all cases the load-strain relationships were linear until the highest load levels were reached.
- (2) At the highest load levels, regions in which the load-strain relationships became non-linear existed for all shells.
- (3) When the load-strain relationships became non-linear the strain-differences were related to the load levels by hyperbolic equations in over 95% of the cases.
- (4) The skin strains were greater than the stringer lip strains at the extremities of all shells, indicating the presence of moments at the shell ends.
- (5) At the lower load levels, the skin strains and the stringer lip strains were substantially the same over the region from 18.0 inches above base to 90 inches



Table XII

Shell D. Strains (micro-inch per inch) at 15% Critical Load

Station 1		Station 2		Station 3		Station 4		Station 5	
Outer	Inner	Outer	Inner	Outer	Inner	Outer	Inner	Outer	Inner
-304	-228	-269	-269	-282	-265	-263	-267	-303	-225
-287	-222	-259	-266	-280	-260	-264	-273	-293	-237
-277	-234	-256	-248	-275	-266	-263	-272	-292	-246
-285	-214	-256	-264	-283	-264	-265	-270	-296	-266
-285	-212	-256	-266	-286	-257	-257	-276	-272	-252
-303	-232	-266	-270	-280	-257	-252	-265	-253	-226
-283	-211	-263	-267	-278	-258	-252	-264	-251	-261
	-197	-254	-260	-275	-265	-255	-259	-269	-253
-297	-216	-261	-265	-276	-266	-253	-266	-257	-258
-290	-251		-266	-273	-265	-263	-263	-263	-259
-294	-249	-254	-259	-273	-264	-246	-254	-261	-272
-285	-252	-254	-257	-269	-265	-256	-268	-282	-261
-299	-246	-261	-260	-281	-263	-267	-264	-273	-277
-296	-238	-265	-270	-284	-271	-252	-268	-311	-262
-284	-214	-263	-261	-279	-270	-271	-283	-349	-265
-298	-215	-265	-268	-273	-264	-261	-265	-292	-265
-300	-227	-264	-270	-285	-264	-254	-275	-278	-194
-305	-208	-268	-270	-281	-266	-260	-278	-294	-171

Table XIII

Shell C. Strains (micro-inch per inch) at 27.4% Critical Load

Station 1		Station 2		Station 3		Station 4		Station 5	
Outer	Inner	Outer	Inner	Outer	Inner	Outer	Inner	Outer	Inner
-413	--	-353	-338	-387	-384	-372	-379	-405	-346
-403	-296	-356	-379	-378	-376	-361	-383	-408	-322
-398	--	-356	-374	-369	-368	-357	-382	-391	-299
-393	-311	-342	--	-378	-371	-370	-372	-394	-322
-391	-307	-358	-381	-382	-381	-359	-368	-389	-476
-303	-299	-362	-368	-376	-370	-351	-371	-371	-333
-413	-311	-354	-368	-374	-363	-358	-364	-379	-348
--	-322	-365	-364	-381	-372	-353	-362	-387	-354
-414	-337	-371	-368	-376	-368	-355	-375	-380	-338
-399	-354	--	-366	-374	-350	-350	-364	-365	-369
-364	-364	-360	-357	-369	-362	-343	-372	-358	-363
-335	-337	-296	-362	-364	-357	-348	-364	-384	-335
-406	-302	-351	-367	-374	-365	-349	-369	-355	-329
-407	-335	-370	-366	-381	-363	-351	-386	-371	-344
-410	-321	-363	-370	-383	-369	-353	-379	-381	-327
-415	-333	-357	-376	-377	-365	-359	-376	-405	-337
-425	-313	-369	-388	-374	-363	-357	-378	-391	-352
-395	-273	-366	-392	-385	-379	-361	-385	-416	-348

Table XIV

Shell A. Strains (micro-inch per inch) at 75% of Critical Load.

Station 1		Station 2		Station 3		Station 4		Station 5	
Outer	Inner	Outer	Inner	Outer	Inner	Outer	Inner	Outer	Inner
-1247	-1016	-1189	-977	-1235	-1214	-1181	-1225	-1249	-1136
-1334	-971	-1164	-1236	-1178	-1234	-1104	-1275	-1292	-1069
-1220	-1026	-1163	-1266	-1211	-1273	-1162	-1182	-1149	-1085
-1296	-1033	-1125	-1219	-1263	-1201	-1114	-1292	-1276	-944
-1324	-1017	-1144	-1240	-1170	-1270	-1191	-1228	-1247	-1200
-1160	-1104	-1150	-1156	-1257	-1177	-1109	-1241	-1159	-1103
-1239	-1010	-1166	-1189	-1154	-1229	-1184	-1196	-1234	-1156
-	-1005	-1132	-1294	-1239	-1213	-1163	-1234	-1255	-1173
-1296	-1111	-1237	-1242	-1296	-1208	-1185	-1182	-1146	-1170
-1358	-996	-	-1279	-1224	-1553	-1149	-1254	-1211	-1145
-1358	-1321	-1128	-1169	-1161	-1221	-1181	-1264	-1241	-1145
-1134	-1043	-1072	-1115	-1315	-1077	-1158	-1195	-1207	-1134
-1312	-916	-1132	-1255	-1176	-1168	-1182	-1250	-1256	-1131
-1394	-985	-1159	-1304	-1223	-1177	-1171	-1250	-1303	-1162
-1216	-1100	-1194	-1239	-1251	-1243	-1153	-1160	-1162	-1204
-1333	-1079	-1160	-1234	-1201	-1216	-1180	-1226	-1236	-1234
-1373	-1017	-1161	-1256	-1180	-1191	-1164	-1217	-1272	-1230
-1195	-1032	-1209	-1213	-1290	-1180	-1148	-1227	-	-1191

Table XV  
Shell B. Strains (micro inch per inch) at 98% of Critical Load

Station 1		Station 2		Station 3		Station 4		Station 5	
Outer	Inner	Outer	Inner	Outer	Inner	Outer	Inner	Outer	Inner
-1915	-1515	-1736	-1846	-1897	-1678	-1757	-1711	-1866	-1675
-1899	-1490	-1675	-1868	-1766	-1795	-1747	-1821	-1871	-1680
-1874	-1644	-1747	-1763	-1989	-1641	-1760	-1743	-1831	-1702
-2024	-1375	-1720	-1869	-1752	-1897	-1724	-1815	-1816	-1591
-1921	-1452	-1719	-1757	-1916	-1555	-1722	-1768	-1878	-1635
-1941	-1368	-1678	-1763	-1825	-1725	-1665	-1768	-1875	-1758
-1889	-1591	-1783	-1793	-1777	-1777	-1800	-1658	-1846	-1782
-1939	-1425	-1682	-1870	-2058	-1739	-1727	-1847	-1948	-1702
-2003	-1410	-1688	-1928	-1681	-1996	-1800	-1877	-1914	-1764
-1928	-1389	—	-1768	-2157	-1505	-1817	-1740	-1895	-1684
-1930	-1333	-1645	-1872	-1629	-1981	-1737	-1820	-1819	-1624
-1843	-1466	-1718	-1714	-1883	-1707	-1689	-1715	-1897	-1649
-1971	-1351	-1699	-1857	-1778	-1758	-1748	-1662	-1778	-1632
-1898	-1357	-1731	-1823	-1893	-1711	-1705	-1718	-1928	-1571
-2001	-1394	-1705	-1829	-1774	-1852	-1749	-1783	-1896	-1575
-1955	-1526	-1821	-1818	-1847	-178	-1740	-1748	-1838	-1518
-1948	-1346	-1661	-1915	-1792	-1711	-1754	-1810	-1925	-1418
-1902	-1504	-1715	-1771	-1719	-1853	-1690	-1796	-1875	-1542

above base. Thus the end moments died out within 18 inches and the central region was under almost pure axial compression.

- (6) As the load levels grew to their highest values there were alternately regions in which the skin strain exceeded the stringer lip strain and regions in which the reverse occurred.
- (7) The strain differences along the panel vertical joint lines were always small.
- (8) There was one region at the mid-height of each shell for which the strain-difference exceeded all others at the highest load levels. At this locality the skin-strain always exceeded the stringer lip strain.

In view of these similarities it might well be conjectured that the buckling behavior of the four shells would be identical. It must be remembered, however, that these are merely qualitative similarities.

A clearer understanding of the instability behavior of the individual shells must come from a more detailed quantitative treatment of the data obtained at the highest load levels. As noted earlier, under these conditions there were a number of strains which were such that the strain differences were related to the load in a hyperbolic fashion. In these cases the Southwell method can be used to estimate the load levels which would correspond to an

infinite strain difference. This has been done for all shells and the results of these computations are presented in Tables XVI through XIX. It is clear from these tables that the lowest values of critical load computed in this manner are always in close agreement with those actually attained. It is equally clear that all the load values which are derived from this non-linear data do not correspond to inward motions. Moreover, the values which are pertinent to an outward motion are most frequently as close or closer in value to the achieved critical load than are those which correspond to an inward motion.

It is well known that shells under axial compression collapse inwards when they become unstable. It is concluded therefore that those elements which are tending to instability outwards can and do act to trigger instability inwards. It would seem likely that when they reach their critical condition and move outwards they are restrained from excessive distortion by the remainder of the shell. Nevertheless, their sudden "yielding" must be accompanied by a sudden redistribution of load over those regions which have not yet reached critical conditions. This redistribution, allied with the stresses induced by the restraining action, then precipitates failure of those elements which are naturally unstable inwards. It seems reasonable to

TABLE XVI. LOCAL STRAIN CONDITIONS AND CRITICAL LOADS DERIVED FROM HIGHEST LOAD LEVEL DATA

SHELL A				
Angle Degrees	Station 2	Station 3	Station 4	Remarks
0	constant	constant	constant	
20	1.190 [o]	constant	1.875 [o]	
40	1.516 [o]	1.243 [o]	* 1.243 [i]	
60	constant	1.163 [i]	1.381 [o]	
80	0.972 [o]	1.608 [o]	1.000 [i]	
100	constant	1.355 [i]	1.275 [o]	
120	1.245 [o]	1.154 [o]	0.999 [i]	
140	1.719 [o]	1.140 [i]	1.402 [o]	COMPLETE
160	0.995 [o]	constant	1.010 [i]	SHELL
180	---	constant	1.177 [o]	
200	1.095 [o]	1.081 [o]	constant	
220	* 1.095 [o]	1.098 [i]	constant	BUCKLED
240	1.147 [o]	1.021 [o]	constant	
260	1.217 [o]	1.521 [i]	1.124 [o]	AND
280	constant	0.991 [o]	constant	
300	1.271 [o]	constant	constant	DAMAGED
320	constant	constant	constant	
340	1.069 [o]	1.448 [i]	1.400 [o]	
Symbols	δ Strain difference * δ reverses in sign ▲ δ changing very rapidly		[o] tending to instability outwards [i] unstable inwards φ has a step change ψ beginning to decrease	
General Note	Local critical load values normalized to actual critical of 233,705 lb.			

TABLE XVII LOCAL STRAIN CONDITIONS AND CRITICAL LOADS DERIVED FROM HIGHEST LOAD LEVEL DATA

SHELL B

Angle Degrees	Station 2	Station 3	Station 4	Remarks
0	1.286 [o]	1.074 [i]	1.040 [i]	No damage
20	1.233 [o]	constant	constant	"
40	constant	1.206 [i]	constant	"
60	1.042 [o]	1.053 [o]	1.118 [o]	"
80	constant	1.193 [i]	constant	"
100	1.040 [o]	constant	1.275 [i]	Damage
120	constant	constant	1.179 [i]	"
140	1.428 [o]	1.061 [i]	1.348 [o]	"
160	1.093 [o]	1.025 [o]	1.050 [o]	"
180	constant	1.075 [i]	0.997 [i]	"
200	1.173 [o]	1.073 [o]	constant	"
220	1.003 [o]	1.158 [i]	constant	"
240	1.267 [o]	constant	constant	"
260	constant	1.255 [i]	constant	"
280	1.138 [o]	0.986 [o]	constant	No damage
300	---	constant	constant	"
320	1.425 [o]	1.135 [i]	constant	"
340	constant	1.017 [o]	constant	"
Symbols	<p>δ Strain difference</p> <p>* δ reverses in sign</p> <p>▲ δ changing very rapidly</p>	<p>[o]</p> <p>[i]</p>	<p>tending to instability outwards</p> <p>unstable inwards</p>	
General Note	Local critical load values normalized to overall critical, 284,281 lb.			



TABLE XVIII LOCAL STRAIN CONDITIONS AND CRITICAL LOADS DERIVED FROM HIGHEST LOAD LEVEL DATA

SHELL C

Angle Degrees	Station 2	Station 3	Station 4	Remarks
0	1.068 [i]	1.031 [i]	erratic	
20	1.112 [o]	1.034 [o]	constant	
40	1.883 [i]	0.961 [o]	1.167 [o]	
60	*▲ [i]	1.028 [i]	linear	
80	1.172 [o]	1.015 [o]	0.982 [o]	
100	1.443 [o]	1.038 [i]	1.096 [o]	
120	*▲ [i]	1.130 [i]	0.997 [i]	COMPLETE
140	1.029 [o]	* developing	1.045 [o]	
160	1.006 [i]	developing	constant	SHELL
180	---	linear	constant	
200	1.142 [o]	0.992 [o]	constant	BUCKLED
220	▲ [o]	1.061 [i]	1.133 [i]	
240	1.220 [o]	0.984 [o]	constant	AND
260	constant	1.063 [i]	1.133 [o]	
280	---	*▲ [o]	constant	DAMAGED
300	constant	1.047 [i]	constant	
320	constant	0.979 [o]	constant	
340	1.142 [o]	linear	erratic	
Symbols	⚬ Strain *⚬ reverses sign ▲ changing very rapidly	⚬ Strain * developing ⚬ linear	[o] tending to instability outwards [i] unstable inwards	
General Note	Local critical load values normalized to actual critical of 255,907 lb.			

TABLE XIX LOCAL STRAIN CONDITIONS AND CRITICAL LOADS DERIVED FROM HIGHEST LOAD LEVEL DATA

S. V.L.D.

Angle Degrees	Station 2	Station 3	Station 4	Remarks
0	δ constant	1.112 [i]	0.994 [c]	No damage
20	"	*Δ [o]	erratic	"
40	"	* [o]	constant	"
60	δ → 0	δ decreasing	*Δ [i]	"
80	δ erratic	1.176 [i]	erratic	"
100	δ = 0	δ linear	linear	Damage
120	δ = 0	1.225 [i]	1.314 [o]	"
140	δ 1.132 [i]	1.012 [o]	constant	"
160	δ erratic	0.993 [o]	---	"
180	---	1.091 [i]	constant	"
200	δ constant	0.975 [o]	1.194 [o]	"
220	---	0.915 [o]	[i]	"
240	1.146 [i]	δ constant	1.400 [o]	"
260	1.117 [o]	1.411 [i]	constant	"
280	0.975 [i]	δ constant	---	No damage
300	δ linear	δ constant	0.968 [i]	"
320	δ constant	1.200 [i]	1.295 [o]	"
340	*Δ [i]	0.980 [o]	1.297 [o]	"
Symbols	δ Strain difference * reverses in sign Δ changing very rapidly	[o] [i]	[o] tending to instability outwards [i] unstable inwards	
General Note	Local critical load values normalized to overall critical, 309,659 lb.			

suggest, in light of the local critical load values and distributions shown in the tables, that this mechanism explains the different behavior patterns exhibited by the shells.

#### 3.7.5 Line-Load Distribution.

The distribution of axial compressive force around the circumference of the shell is directly associatable with the circumferential distribution of centroidal strain. Calculations of the centroidal strains over the entire spectrum of loading show that remarkably uniform distributions were achieved in all cases. This is illustrated clearly in Tables XIX through XXIII. In these tables the values of the centroidal strain are given at the 18 stations around the circumference for each of the 5 longitudinal measurement positions. For added clarity these strain values have been normalized to the mean value for the shell as a whole. Each table is pertinent to a different shell, but in each case the load level quoted is of the order of 75% critical.

It is interesting to note that, when the full set of values for each shell are considered as a family, the cumulative totals versus specific strain level plot as a straight line on probability paper. This implies that the

TABLE XX.

## SHELL A. CENTROIDAL STRAINS.

## Local Centroidal Strains Normalized to Mean

Angle (°)	Station 1	Station 2	Station 3	Station 4	Station 5
0	0.983	0.944	1.026	0.998	1.014
20	1.022	0.983	0.998	0.966	1.022
40	0.970	0.998	1.027	0.976	0.943
60	1.016	0.964	1.039	0.976	0.981
80	1.028	0.980	1.002	1.004	1.030
100	0.955	0.962	1.030	0.960	0.954
120	0.977	0.980	0.983	0.992	1.011
140	1.080	0.987	1.028	0.993	1.027
160	1.035	1.034	1.061	0.989	0.963
180	1.065	---	1.029	0.986	0.995
200	1.048	0.953	.985	1.007	1.012
220	0.924	0.906	1.037	0.977	0.990
240	0.995	0.977	0.985	1.005	1.017
260	1.060	1.005	1.009	0.998	1.052
280	0.986	1.009	1.043	0.970	0.946
300	1.049	0.988	1.007	0.997	1.032
320	1.056	0.996	0.986	0.986	1.052
340	0.957	1.012	1.049	0.979	-----

TABLE XXI.

SHELL B. CENTROIDAL STRAINS

Local Centroidal Strains Normalized to Mean

Angle (°)	Station 1	Station 2	Station 3	Station 4	Station 5
0	1.007	0.997	1.010	0.971	1.001
20	0.990	0.974	1.002	0.984	1.007
40	1.019	0.980	1.035	0.980	1.000
60	1.028	0.992	1.021	0.984	0.976
80	0.998	0.967	1.010	0.976	1.025
100	0.990	0.966	1.004	0.964	1.036
120	1.016	0.993	1.013	0.984	1.039
140	1.002	0.977	1.053	1.001	1.045
160	1.022	0.996	1.042	1.025	1.046
180	1.007	---	1.065	1.002	1.017
200	0.980	0.967	1.009	0.981	----
220	0.966	0.959	1.015	0.964	1.021
240	1.002	0.989	1.004	0.975	0.993
260	0.993	0.991	1.026	0.971	1.024
280	1.023	0.996	1.023	0.989	1.003
300	1.027	1.019	1.033	0.984	0.976
320	0.991	0.981	0.988	0.994	0.989
340	0.994	0.970	0.996	0.968	0.984

TABLE XXII.

SHELL C. CENTROIDAL STRAINSLocal Centroidal Strains Normalized to Mean

Angle (°)	Station 1	Station 2	Station 3	Station 4	Station 5
0	---	---	1.050	1.015	1.034
20	0.982	0.980	1.007	0.980	1.013
40	---	0.975	1.004	1.001	0.997
60	0.996	---	1.030	0.993	0.997
80	0.986	0.998	1.020	0.981	0.969
100	0.959	0.985	1.010	0.956	0.990
120	1.019	0.964	0.986	0.959	0.957
140	---	0.982	1.017	0.937	0.976
160	1.044	0.998	1.010	0.982	0.995
180	1.049	---	1.014	0.971	0.976
200	0.993	0.982	1.011	0.953	0.950
220	---	---	1.003	0.975	0.995
240	1.015	0.973	1.018	0.992	0.934
260	1.038	1.009	1.041	1.000	0.993
280	1.030	1.002	1.043	0.998	1.022
300	1.056	0.989	1.031	1.006	1.039
320	1.021	1.025	1.018	1.000	1.039
340	0.992	1.024	1.056	1.013	1.057

TABLE XXIII.

SHELL D. CENTROIDAL STRAINSLocal Centroidal Strains Normalized to Mean

Angle (°)	Station 1	Station 2	Station 3	Station 4	Station 5
0	1.03	1.009	1.039	1.011	1.089
20	0.984	0.971	1.028	1.003	1.038
40	0.976	0.953	1.025	0.990	1.033
60	0.979	0.969	1.037	1.004	1.045
80	0.995	0.974	1.043	0.993	1.017
100	0.952	0.998	1.016	0.966	0.974
120	0.965	0.988	1.006	0.962	0.991
140	---	0.953	1.010	0.947	0.985
160	0.981	0.982	1.018	0.962	0.988
180	1.016	---	1.020	0.977	0.974
200	1.017	0.955	1.014	0.951	1.007
220	0.990	0.959	1.005	0.980	1.030
240	1.018	0.977	1.032	1.002	1.057
260	1.025	0.992	1.058	1.005	1.067
280	0.991	0.999	1.046	0.996	-----
300	1.009	1.008	1.016	0.986	1.013
320	1.027	0.987	1.051	0.981	1.018
340	1.054	1.004	1.038	1.000	0.998

variations which are experienced are of a random character. The smallness of the coefficients of variation lead to the opinion that it would be extremely difficult indeed to achieve closer correspondence.

#### 3.7.6. Load-Displacement Histories.

A large amount of data on the motions of the shell walls induced by loading was acquired. This data has not yet been completely analyzed. The analysis which has been made does not, however, show any unexpected trends or behavior patterns.

#### 4. Conclusions

The studies which were made with small scale plastic shells showed clearly that non-destructive methods of evaluation of axially compressed cylindrical shells are feasible. The experience with the large scale vehicles indicates, however, that if such techniques are to be applied to large scale testing the loading and probing system must be designed to work in unison from the onset.

The work on large scale cylindrical shells shows that vehicles with excellent quality of geometric form can be fabricated. It demonstrates, too, that provided sufficient care is exercised in the fabrication of the



loading devices, and in the machining of the ends of the specimens, excellent control of load distribution can be attained.

### References

- (1) Arbocz, J., "The Effect of General Imperfections on the Buckling of Cylindrical Shells." Ph. D. Thesis, California Institute of Technology, Pasadena, 1968.
- (2) Babcock, D. D., "The Buckling of Cylindrical Shells With an Initial Imperfection Under Compression Loading." Ph. D. Thesis California Institute of Technology, Pasadena, 1962.
- (3) Katz, L. "Compression Tests on Integrally Stiffened Cylinders." N.A.S.A. TM X 53315, 1965.
- (4) Weller, T., and Singer, J., "Experimental Studies on Buckling of 7075-T6 Aluminum Alloy Integrally Stringer-Stiffened Shells." TAE report No. 135. Israel Institute of Technology, Haifa, 1971.
- (5) Babcock, D. C., "Experiments in Shell Buckling." Section 14, Thin Shell Structures. Fung, Y. C., Ed., and Sechler, E.E. Ed., Prentice Hall, Inc., Englewood Cliffs, N. J., 1974.
- (6) Horton, W. H., Singhal, M.K., and Haack, T. A., "The Use of Models in Structural Testing." Instrumentation in the Aerospace Industry, ASI 72231, pp. 159-164. Instrument Society of America, Pittsburg, Pennsylvania, 1972.
- (7) Haack, T. A., "The Development of New Techniques for the Manufacture and Testing of Cylindrical Shells." Master's Thesis Georgia Institute of Technology, Atlanta, Georgia. March, 1973.

- (8) Ford, J. S. III, "Parametric Studies on the Stability of Stringer and Ring Reinforced Shells." Ph. D. Thesis, Georgia Institute of Technology, November, 1970.
- (9) Donnell, L. H., "On the Application of Southwell's Method for the Analysis of Buckling Tests.", Stephen Timoshenko 60th Anniversary Volume, McGraw-Hill Book Co., 1938, pp. 2730.
- (10) Tuckerman, L. B., "Hetrostatic Loading and Critical Astatic Loads," National Bureau of Standards Research Paper RP 1163, Journal of Research, N.B.S., 22, 1939, pp. 27-38.
- (11) Craig, J. I., "An Experimental Study of Wall Motions in Circular Cylindrical Shells Under Combined Loadings." Ph. D. Thesis, Stanford University, Stanford, California, 1969.
- (12) Bank, M. H. II, "Some Discussions on the Stability of Structural and Mechanical Systems." Ph. D. Thesis, Georgia Institute of Technology, Atlanta, Georgia, August, 1971.
- (13) Singhal, M. K., "Studies on the Elastic Stability of Bodies." Ph. D. Thesis, Georgia Institute of Technology, Atlanta, Georgia, 1973.
- (14) Nassar, E. E., "On the Dynamic Characteristics of Beams, Plates and Shells." Ph. D. Thesis, Georgia Institute of Technology, Atlanta, Georgia, 1973.
- (15) Horton, V. H., Singhal, M. K., and Nassar, E. E., "On the Non-Destructive Determination of the Critical Loads for Shell Bodies." To be published by the SEFA in Experimental Mechanics.

- (16) Duggan, M. F., "A Study of the Effects of Geometric Imperfection Upon the Stability Behavior of Cylindrical Shells Under Axial Compression." Master's Thesis, Georgia Institute of Technology, Atlanta, Georgia, December, 1971.
- (17) Craig, J. I., and Duggan, M. F., "Non-Destructive Shell Stability Estimation by a Combined Loading Technique." Experimental Mechanics, Volume 3, p. 381-387, September, 1973.
- (18) Peterson, J. P., "Buckling of Stiffened Cylinders in Axial Compression and Bending - A Review of Test Data." NASA TN-556;. ;970.
- (19) Arbocz, J., and Babcock, C. D., "Experimental Investigation of General Imperfections on the Buckling of Cylindrical Shells." California Institute of Technology. Galcit Report SM 68-7, 1968.
- (20) Horton, W. H., and Craig, J. I., "Experimental Studies on the Effect of General Imperfections on the Elastic Stability of Thin Shells," Israel Journal of Technology, 7, (1-2), 91-103, 1969.
- (21) Singer, J., Arbocz, J., and Babcock, D. D. Jr., "Buckling of imperfect Stiffened Cylindrical Shells Under Axial Compression." Proceedings of the AIAA/ASME 11th Structures, Structural Dynamics, and Materials Conference, April, 1970.
- (22) Block, D. I., Cord, M. F., and Mikulas, M. M. Jr., "Buckling of Eccentrically Stiffened Orthotropic Cylinders." N.A.S.A. TN D. 2960, 1965.

- (23) Craig, J. I., Bailey, S. C., and Horton, W. H., "Non-Destructive Stability Evaluation of Large Shell Structures by Direct Computer Controlled Testing." Instrumentation in the Aerospace Industry ASI 72231. pp. 165-172. Instrument Society of America, Pittsburg, Pennsylvania, 1972.
- (24) Arthur, M. F. "Initial Imperfection Measurement of Large Scale Cylindrical Shells." Graduate Special Problem. Georgia Inst. of Tech. Unpublished.